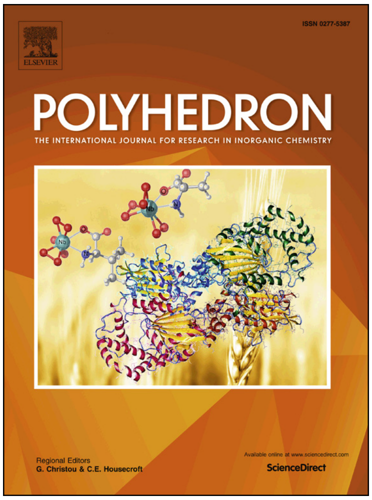

A planar anthracene–imidazolium / anthracene-benzimidazolium cation system in a spherical polyoxometalate matrix: synthesis, crystallography and spectroscopy

Tanmay Chatterjee, Tanmaya Kumar, Samar K. Das

PII: S0277-5387(17)30086-4
DOI: http://dx.doi.org/10.1016/j.poly.2017.01.049
Reference: POLY 12453

To appear in: *Polyhedron*

Received Date: 24 November 2016
Revised Date: 26 January 2017
Accepted Date: 28 January 2017

Please cite this article as: T. Chatterjee, T. Kumar, S.K. Das, A planar anthracene–imidazolium / anthracene-benzimidazolium cation system in a spherical polyoxometalate matrix: synthesis, crystallography and spectroscopy, *Polyhedron* (2017), doi: http://dx.doi.org/10.1016/j.poly.2017.01.049

A planar anthracene–imidazolium / anthracene-benzimidazolium cation system in a spherical polyoxometalate matrix: synthesis, crystallography and spectroscopy

Tanmay Chatterjee, Tanmaya Kumar and Samar K. Das*

School of Chemistry, University of Hyderabad, Hyderabad 500 046, India

---

Supplementary data associated with this article can be found, in the online Version, at xxxxxxxxxxxxxxxxxxxx

Corresponding author. Tel: +91-40-2301-1007; fax: +91-40-2301-2460.
E-mail address: skdsc@uohyd.ernet.in (S. K. Das)

Abstract

A series of ion–pair compounds, comprising of Lindqvist type isopolyanions *viz.*, $[Mo_6O_{19}]^{2-}$ and $[W_6O_{19}]^{2-}$ as the counter anions and anthracene–imidazolium / anthracene-benzimidazolium as counter cations, have been described. Structures of the isolated stoichiometric solids have been unambiguously determined by single crystal X–ray diffraction analysis. In spite of the structural incompatibility between anthracene (planar) and the present polyoxometalate anions (spherical), coulombic and several intermolecular weak interactions, e.g. C–H···O, C–H···π, π–π etc. compensate the destabilization energy raised due to presence of the structurally mis-matched components in the respective crystal lattices. Single-crystal- as well as powder X-ray-diffraction (PXRD) analyses reveal iso-structural relationship between the hexamolybdates- and hexatungstates-associated ion pair compounds. Conformational variation has been observed in the crystal structures containing benzyl benzimidazolium counter cations. Diffuse reflectance electronic absorption spectral studies are performed to understand the relatively intense color of the title compounds in their solid states in comparison to their respective solution states.

Keywords: Lindqvist isopolyanions / Coulombic interactions / Supramolecular interactions / Stoichiometric solids / Conformational variation / Solid state electronic spectral studies

1. Introduction

The term 'co-crystal', in a broader sense, denotes crystalline solids made from more than one component held together by non–covalent intermolecular interactions. To–date, many authors have defined the term in diverse ways although an accurate and universally accepted definition of 'co-crystal' is not yet available [1]. Another characteristic feature of the co-crystals is that they exhibit distinct physical properties (for example, solubility, thermal stability, melting point *etc.*) than those of the co-crystal formers. Thus, after the intermolecular association of more than one molecular component (not necessarily to be both solids), a crystalline solid (necessarily to be solid) is formed, where the uniqueness / identity of the constituents disappears and a modulation of their physico–chemical properties (in solution state there might be a retention of their individuality) is observed [2].

Very often, in the case of co-crystals, a central molecule is focused which is co-crystallized with various other secondary components (called as conformers [3]). At this point, it should be remembered that, co-crystals do not involve only organic molecules, but also ionic compounds, inorganic compounds / complexes as co-formers. The first co-crystal (all organic) was discovered by Wohler (1844) in the *era* before the invention of X–ray by Rontgen (1895) [4-5]. Since then co-crystals turned out to be a subject of immense interest and at present, majority of the co-crystals, reported in literature, incorporate active pharmaceutical ingredients (APIs) as one component in achieving bioactive materials [6-8]. Besides co-crystals obtained from only neutral hosts or guests, ionic compounds are also found to form co-crystals with definite stoichiometry. Few representative examples include co-crystals containing both carboxylic acid and acid salt, phenolic acid and acid salt or organic–inorganic co-crystals [3].

Several intermolecular forces, for example, hydrogen bonding, van der Walls, electrostatic, π–stacking *etc.* govern molecular packing of the crystallizing substances in a crystal lattice. The central aim of the supramolecular chemistry is to gain organized arrangement / packing of the molecules in a crystal using these intermolecular interactions [9]. Apart from the co-crystals built from simple organic:organic or organic: inorganic molecular components, recent interests have been grown to incorporate complex molecular systems such as, molecules with curved and flat external surfaces in the crystal lattice. Obtaining multi-dimensional and/or larger supramolecular ensembles using fullerenes as the crystallizing substances has become a subject of extensive research to the structural chemists / crystallographers since the last two decades. The ubiquitous three–dimensional and higher symmetrical shape of the fullerenes along with their exciting physical and chemical properties (e.g., their facile electron accepting abilities) have drawn significant attention to the structural chemists for choosing them as good candidates to build complex supramolecular architectures [10-16] .

Polyoxometalates (POMs), on the other hand, are transition metal–oxide based cluster anions comprising of metal ions bridged by oxygen atoms [17], which have received an enormous attention by the contemporary chemists, because of their diverse physical and chemical properties e.g., diversity in their shape, size, electrochemistry, acid–base chemistry, charge distribution *etc.* including their participation in soft-oxometalate (SOM) chemistry [18-21]. The surface of these macro–anions bearing oxygen atoms, are of particular interest. Interestingly, some features of the POM anions resemble that of the fullerenes *e.g.* (i) their electron accepting nature [22] (the metal centers are in their higher oxidation states and thus can be partially reduced by a secondary substance), (ii) their highly symmetrical shape *etc.* Therefore, they can be introduced in supramolecular chemistry as the low–cost alternative to the fullerenes despite the fact, that the POM anions have profound chances to form dative linkages to the external metal centers (thus acting as ligands) *via* the terminal oxygen atoms [23]. Crystallization of the POM anions with supramolecular complexes of the macrocyclic systems [24-25] or other counter cations [26] have been documented in literature that illustrate the usage of the POM anions as building blocks in the context of crystal engineering. However, co-crystallization of the POM anions with π–donor flat aromatic co-formers is of great crystallographic challenge due to size incompatibility between the interacting components. Aromatics containing flat π surfaces (e.g. anthracene, pyrene, *etc.*) can interact with the surface of the POM anions *via* two possible ways as depicted in Scheme 1. The planar aromatics mostly pack with each other through π–staking interactions in their crystals. These π–staked aromatics could further associate with the POM macroanions through C–H···O hydrogen bonding interactions as shown in Scheme 1a. Thus, in this way of interaction, there are no direct contacts between the π cloud of the aromatics and the POM anions. The other interaction mode, as shown in Scheme 1b, demonstrates direct contact between the π surface of the flat aromatics and the electron accepting POM surfaces, thereby including possibility of charge transfer interaction between the components that result in partial oxidation and partial reduction of the aromatics and the POM anions respectively.

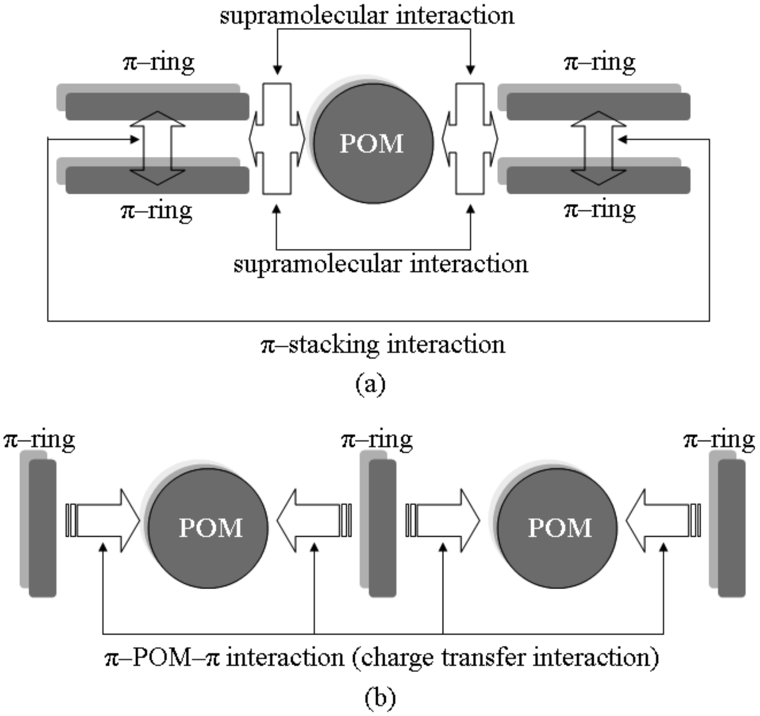

Scheme 1. Two possible ways of interactions between flat aromatics and POMs.

Kochi and co-workers first reported the π···POM interactions in a series of co-crystals, made up of anthracene or pyrene based conformers [27]. The relevant publication comments that, coulombic interactions between the POM anions and the alkylammonium or pyridinium groups, attached to the polyaromatic hydrocarbons (anthracene and pyrene) *via* flexible polymethylene chains, help the planar surfaces of the aromatics to come closer to the POM surfaces, thus involving in the π···POM interactions. This has led to charge transfer from the π–donors to the POM anions [27]. Similarly, Tan and Bu reported four hybrid compounds, formed by electrostatic interactions between the POM and the anthracene donor having two alkylimidazolium groups, that can be described as charge-transfer salts. They calculated the energy level parameters, which reasonably matched with those of the commonly used organic electroluminescence devices [28]. Keeping these works in mind, a series of hexamolybdate and hexatungstate (iso-polyanions) based ion–pair compounds (Scheme 2: **10a**-**f**, **11a**-**f**, **12a**-**e**, **13a**-**e**), which contain anthracene–imidazolium or anthracene–benzimidazolium species as counter cations, have been synthesized and reported in this article.

We wish to analyze the structural and physical properties of the ion-pair compounds, **10a**-**f**, **11a**-**f**, **12a**-**e**, **13a**-**e** (Scheme 2), constructed from anthracene-based counter cations bearing a heavy atom (Br) at the 9th position of anthracene and polyoxometalate (POM) anions $[M^{VI}_6O_{19}]^{2-}$ (M = Mo and W). Coulombic association between the POM anion surfaces and the imidazolium or benzimidazolium cationic counterparts have been observed whereas, the anthracene moieties are involved in C–H···O, C–H···π or π···π interactions to optimize the

(a) (b)

R= Me (**10a**, **11a**), n-Pr (**10b**, **11b**),
i-Pr (**10c**, **11c**), n-Bu (**10d**, **11d**),
hexyl (**10e**, **11e**),decyl (**10f**, **11f**)

$R_1 = R_2 = R_3 = R_4 = R_5$ = H (**12a**, **13a**)
R_1 = F, $R_2 = R_3 = R_4 = R_5$ = H (**12b**, **13b**)
R_1 = Cl, $R_2 = R_3 = R_4 = R_5$ = H (**12c**, **13c**)
R_1 = Br, $R_2 = R_3 = R_4 = R_5$ = H (**12d**, **13d**)
$R_1 = R_2 = R_3 = R_4 = R_5$ = Me (**12e**, **13e**)

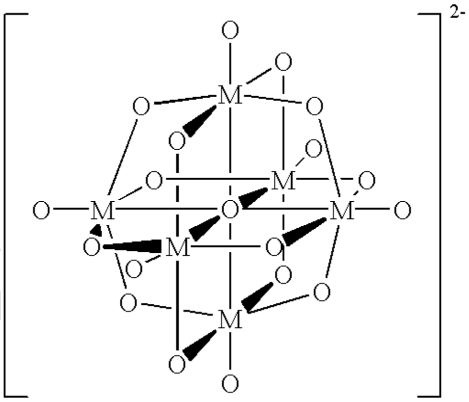

(c)

Scheme 2. (a) Anthracene-imidazolium ion-pair compounds (**10a-f, 11a-f**), (b) the anthracene-benzimidazolium ion-pair compounds (**12a-e, 13a-e**), (c) the structural representation of hexametalateate ion, $[Mo_6O_{19}]^{2-}$.

lattice energy. We found that varying the alkyl chain length of the imidazolium cation (**10a**-**f**, **11a**-**f**: Scheme 2) or changing the substituents in benzimidazolium moieties (**12a**-**e**, **13a**-**e**: Scheme 2) causes a modification in hydrogen bonding situation to some extent, whereas in the all the crystals, the nature of the π···π stacking interaction remains invariant. The remaining part of this article deals with the detailed structural analysis and solid state absorption spectroscopy of the title compounds that are electro–neutral in nature.

2. Experimental

2.1. Materials and physical methods

All the chemicals were received as reagent grade and used without any further purification.

2.2 Characterization:

Elemental analyses were determined by FLASH EA series 1112 CHNS analyzer. Infrared spectra of solid samples were obtained as KBr pellets on a JASCO-5300 FT-IR spectrophotometer. Powder X-ray diffraction patterns were recorded on a Bruker D8-Advance diffractometer using graphite monochromated CuKα1 (1.5406 Å) and Kα2 (1.54439 Å) radiations. The electronic absorption spectra have been recorded on a Cary 100 Bio UV−visible spectrophotometer at room temperature. ^{1}H NMR spectra have been recorded in a Bruker AV 400 MHz spectrometer. The chemical shifts (δ) are reported in ppm with respect to the solvent signals. Solution mass spectra (LCMS) were obtained on a LCMS-2010A Shimadzu spectrometer.

Synthesis.

*9–bromo–10–(bromomethyl)anthracene (**2**).* Bromine (2 equivalents) was added drop wise to a stirred solution of triphenylphosphine (1 equivalent) in acetonitrile at room temperature and the pale yellow slurry was stirred for 15 min. Solid 9–anthracene methanol (1 equivalent) was then added slowly and the reactants were allowed to react at room temperature until total consumption of the starting material (TLC) after which, it was refrigerated overnight. The product, which appeared as yellow precipitate, was isolated by filtration, washed with little cold methanol and then dried under vacuum. It was further re–crystallized twice from chloroform before use. Characterization data completely corroborated with the literature reported data [29].

*General procedure for the synthesis of the N–alkyl imidazoles (**4a–f**) and N–benzyl benzimidazoles (7a–e).* Imidazole (**3**) / benzimidazole (**5**) (10 mmol) was dissolved in 10 ml of DMSO and solid NaOH (15 mmol) was then added it. The resulting pale yellow suspension was stirred in air at room temperature for 1.5 h, after which, the alkyl bromides or benzyl chlorides (15 mmol) were added and allowed to react until completion (TLC). Water (50 ml) was then added and the products were extracted with ethyl acetate. Combined organic layers were washed several times with water, then with brine, dried over Na_2SO_4 and subjected to chromatographic purification over silica (100–200 mesh) using MeOH : EtOAc 5:95 (v/v) as the mobile phase. Compounds **4a**–**f** were isolated as yellow oils whereas, the compounds **7a**–**e** were white solid. Spectroscopic data of the N–alkyl imidazoles are in accord with earlier literature and thus haven't shown here [30].

*N–benzyl–benzimidazole (**7a**).* White solid; Yield = 77%; ^{1}H NMR (400 MHz, $CDCl_3$, TMS) δ: 7.92 (s, 1H), 7.84 (d, J = 8 Hz, 1H), 7.21–7.37 (m, 6H), 7.15 (d, J = 8 Hz, 2H), 5.29 (s, 2H). ^{13}C NMR (100 MHz, $CDCl_3$, TMS) δ: 143.9, 143.3, 135.5, 133.9, 129.0, 128.3, 127.0, 123.1, 120.4, 110.1, 48.8. LC–MS (positive mode) m/z = 209 $(M^{+}+H)^{+}$. Anal. Calcd. For $C_{14}H_{12}N_2$ (208.26): C, 80.74; H, 5.81; N, 13.45. Found: C, 80.72; H, 5.84; N, 13.44.

*N–(4–fluorobenzyl)–benzimidazole (**7b**).* Off–white solid; Yield = 73%; ^{1}H NMR (400 MHz, $CDCl_3$, TMS) δ: 7.91 (s, 1H), 7.76–7.82 (m, 1H), 6.90–7.33 (m, 7H), 5.26 (s, 2H). ^{13}C NMR (100 MHz, $CDCl_3$, TMS) δ: 163.7, 161.3, 143.9, 143.1, 131.2, 128.9, 123.2, 122.4, 120.4, 116.1, 115.9, 110.0, 48.1. LC–MS (positive mode) m/z = 227 $(M^{+}+H)^{+}$. Anal. Calcd. For $C_{14}H_{11}FN_2$ (226.25): C, 74.32; H, 4.90; N, 12.38. Found: C, 74.36; H, 4.87; N, 12.41.

*1–(4–chlorobenzyl)–benzimidazole (**7c**).* Off–white solid; Yield = 73%; ^{1}H NMR (400 MHz, $CDCl_3$, TMS) δ: 8.05 (s, 1H), 7.82 (m, 2H), 7.00–7.37 (m, 6H), 5.30 (s, 2H). ^{13}C NMR (100 MHz, $CDCl_3$, TMS) δ: 143.3, 142.9, 134.2, 133.9, 133.5, 129.2, 128.4, 123.4, 122.7, 120.2, 110.1, 48.3. LC–MS (positive mode) m/z = 244 $(M^{+}+H)^{+}$. Anal. Calcd. For $C_{14}H_{11}ClN_2$ (242.70): C, 69.28; H, 4.57; N, 11.54. Found: C, 69.27; H, 4.53; N, 11.57.

*N–(4–bromobenzyl)–benzimidazole (**7d**).* Pale–yellow solid; Yield = 75%; ^{1}H NMR (400 MHz, $CDCl_3$, TMS) δ: 7.92 (s, 1H), 7.83 (d, J = 8 Hz, 1H), 7.43 (d, J = 8 Hz, 2H), 7.23–7.28 (m, 3H), 7.01 (d, J = 8 Hz, 2H), 5.26 (s, 2H). ^{13}C NMR (100 MHz, $CDCl_3$, TMS) δ: 143.9, 143.1, 134.5, 133.7, 132.2, 128.7, 123.3, 122.3, 120.5, 109.9, 48.2. LC–MS (positive mode) m/z = 288 $(M^{+}+H)^{+}$. Anal. Calcd. For $C_{14}H_{11}BrN_2$ (287.15): C, 58.56; H, 3.86; N, 9.76. Found: C, 58.55; H, 3.83; N, 9.80.

*N–(2,3,4,5,6–pentamethylbenzyl)–benzimidazole (**7e**).* White solid; Yield = 78%; ^{1}H NMR (400 MHz, $CDCl_3$, TMS) δ: 7.87 (s, 1H), 7.20–7.63 (m, 4H), 5.33 (s, 2H), 2.14–2.38 (m, 15H). ^{13}C NMR (100 MHz, $CDCl_3$, TMS) δ: 144.2, 142.0, 136.2, 134.2, 133.5, 127.2, 122.8, 122.3, 120.4, 109.6, 44.4, 17.2, 16.9, 16.6. LC–MS (positive mode) m/z = 279 $(M^{+}+H)^{+}$. Anal. Calcd. For $C_{19}H_{22}N_2$ (278.39): C, 81.97; H, 7.97; N, 10.06. Found: C, 81.93; H, 7.99; N, 10.08.

*General procedure for the synthesis of the ANT–Im or ANT–BenzIm bromide salts (**8a–f** and **9a–e**).* A mixture of 9–bromo–10–(bromomethyl)anthracene (**2**) (1 mmol) and the relevant N–alkyl imidazoles (**4a**–**f**) or N–benzyl benzimidazoles (**7a**–**e**) in THF (15 ml) was refluxed at open condition for 24 h. By this time the products **8a**–**f** and **9a**–**e** appeared as yellow precipitates which were isolated by filtration, washed with little THF, then with ether and were air–dried. Yield: 85–89% (imidazolium salts) and 80–87% (benzimidazolium salts).

*Bromide **8a***. Yellow solid. Anal. Calcd. For $C_{19}H_{16}Br_2N_2$ (432.25): C, 52.81; H, 3.73; N, 6.48. Found: C, 52.76; H, 3.75; N, 6.51.

*Bromide **8b***. Yellow solid. Anal. Calcd. For $C_{21}H_{20}Br_2N_2$ (460.20): C, 54.81; H, 4.38; N, 6.09. Found: C, 54.82; H, 4.36; N, 6.05.

*Bromide **8c***. Yellow solid Anal. Calcd. For $C_{21}H_{20}Br_2N_2$ (460.20): C, 54.81; H, 4.38; N, 6.09. Found: C, 54.84; H, 4.37; N, 6.07.

*Bromide **8d***. Yellow solid. Anal. Calcd. For $C_{22}H_{22}Br_2N_2$ (474.23): C, 55.72; H, 4.68; N, 5.91. Found: C, 55.74; H, 4.71; N, 5.89.

*Bromide **8e***. Yellow solid. Anal. Calcd. For $C_{24}H_{26}Br_2N_2$ (502.28): C, 57.39; H, 5.22; N, 5.58. Found: C, 57.37; H, 5.16; N, 5.60.

*Bromide **8f***. Yellow solid. Anal. Calcd. For $C_{28}H_{34}Br_2N_2$ (558.39): C, 60.23; H, 6.14; N, 5.02. Found: C, 60.27; H, 6.11; N, 4.98.

*Bromide **9a***. Yellow solid. Anal. Calcd. For $C_{29}H_{22}BrClN_2$ (513.86): C, 67.78; H, 4.32; N, 5.45. Found: C, 67.80; H, 4.27; N, 5.37.

*Bromide **9b***. Yellow solid. Anal. Calcd. For $C_{29}H_{21}BrClFN_2$ (531.85): C, 65.49; H, 3.98; N, 5.27. Found: C, 65.51; H, 3.99; N, 5.26.

*Bromide **9c***. Yellow solid. Anal. Calcd. For $C_{29}H_{21}BrCl_2N_2$ (548.30): C, 63.53; H, 3.86; N, 5.11. Found: C, 63.56; H, 3.84; N, 5.13.

*Bromide **9d***. Yellow solid. Anal. Calcd. For $C_{29}H_{21}Br_2ClN_2$ (592.75): C, 58.76; H, 3.57; N, 4.73. Found: C, 58.79; H, 3.55; N, 4.72.

*Bromide **9e***. Yellow solid. Anal. Calcd. For $C_{34}H_{32}BrClN_2$ (583.99): C, 69.93; H, 5.52; N, 4.80. Found: C, 69.96; H, 5.53; N, 4.73.

*General Procedure for the synthesis of ion-pair complexes (**10 a-f, 11 a-f, 12 a-e, 13 a-e**).* To a stirred solution of salts **8 a-f** or **9 a-e** (2 mmol) in acetonitrile is added the hexametalate salt (1 mmol), to give an immediate precipitate, which is further stirred for 30-45 mins. at room temperature. The molybdate salts (**10 a-f**, **12 a-e**) were orange in colour, while the tungstate salts (**11a-f**, **13 a-e**) precipitated as yellow salts. They were then filtered and then air dried.

*Hexamolybdate **10a***. Orange yellow solid. IR (KBr, cm^{-1}): 3144.25 (C–H), 3097.96 (C–H), 956.78 (Mo=O), 898.91 (Mo–O–Mo). Anal. Calcd. For $C_{38}H_{32}Br_2N_4Mo_6O_{19}$ (1584.12): C, 28.81; H, 2.04; N, 3.54. Found: C, 28.66; H, 1.99; N, 3.61.

Hexamolybdate ***10b***. Orange yellow solid. IR (KBr, cm^{-1}): 3152.17 (C–H), 3070.29 (C–H), 954.87 (Mo=O), 895.11 (Mo–O–Mo). Anal. Calcd. For $C_{42}H_{40}Br_2N_4Mo_6O_{19}$ (1640.23): C, 30.75; H, 2.46; N, 3.42. Found: C, 30.41; H, 2.39; N, 3.53.

Hexamolybdate ***10c***. Orange yellow solid. IR (KBr, cm^{-1}): 3145.19 (C–H), 3092.58 (C–H), 949.19 (Mo=O), 890.17 (Mo–O–Mo). Anal. Calcd. For $C_{42}H_{40}Br_2N_4Mo_6O_{19}$ (1640.23): C, 30.75; H, 2.46; N, 3.42. Found: C, 30.57; H, 2.44; N, 3.56.

Hexamolybdate ***10d***. Orange yellow solid. IR (KBr, cm^{-1}): 3141.15 (C–H), 3089.91 (C–H), 958.78 (Mo=O), 897.41 (Mo–O–Mo). Anal. Calcd. For $C_{44}H_{44}Br_2N_4Mo_6O_{19}$ (1668.28): C, 31.68; H, 2.66; N, 3.36. Found: C, 31.63; H, 2.63; N, 2.42.

Hexamolybdate ***10e***. Orange yellow solid. IR (KBr, cm^{-1}): 3157.33 (C–H), 3068.97 (C–H), 941.48 (Mo=O), 891.96 (Mo–O–Mo). Anal. Calcd. For $C_{48}H_{52}Br_2N_4Mo_6O_{19}$ (1724.39): C, 33.43; H, 3.04; N, 3.25. Found: C, 33.35; H, 3.01; N, 3.30.

Hexamolybdate ***10f***. Orange yellow solid. IR (KBr, cm^{-1}): 3162.19 (C–H), 3091.17 (C–H), 957.12 (Mo=O), 893.22 (Mo–O–Mo). Anal. Calcd. For $C_{56}H_{68}Br_2N_4Mo_6O_{19}$ (1836.60): C, 36.62; H, 3.73; N, 3.05. Found: C, 36.53; H, 3.71; N, 3.12.

Hexatungstate ***11a***. Yellow solid. IR (KBr, cm^{-1}): 3150.04 (C–H), 3092.17 (C–H), 978.00 (W=O), 802.46 (W–O–W). Anal. Calcd. For $C_{38}H_{32}Br_2N_4W_6O_{19}$ (2111.52): C, 21.62; H, 1.53; N, 2.65. Found: C, 21.59; H, 1.51; N, 2.68.

Hexatungstate ***11b***. Yellow solid. IR (KBr, cm^{-1}): 3157.12 (C–H), 3076.49 (C–H), 982.54 (W=O), 799.35 (W–O–W). Anal. Calcd. For $C_{42}H_{40}Br_2N_4W_6O_{19}$ (2167.63): C, 23.27; H, 1.86; N, 2.58. Found: C, 23.22; H, 1.83; N, 2.62.

Hexatungstate ***11c***. Yellow solid. IR (KBr, cm^{-1}): 3147.97 (C–H), 3096.19 (C–H), 982.88 (W=O), 789.79 (W–O–W). Anal. Calcd. For $C_{42}H_{40}Br_2N_4W_6O_{19}$ (2167.63): C, 23.27; H, 1.86; N, 2.58. Found: C, 23.24; H, 1.81; N, 2.65.

Hexatungstate ***11d***. Yellow solid. IR (KBr, cm^{-1}): 3148.83 (C–H), 3043.27 (C–H), 988.72 (W=O), 801.91 (W–O–W). Anal. Calcd. For $C_{44}H_{44}Br_2N_4W_6O_{19}$ (2195.68): C, 24.07; H, 2.02; N, 2.55. Found: C, 24.03; H, 2.00; N, 2.61.

Hexatungstate ***11e***. Yellow solid. IR (KBr, cm^{-1}): 3142.26 (C–H), 3045.27 (C–H), 979.89 (W=O), 800.22 (W–O–W). Anal. Calcd. For $C_{48}H_{52}Br_2N_4W_6O_{19}$ (2251.79): C, 25.60; H, 2.33; N, 2.49. Found: C, 25.51; H, 2.30; N, 2.52.

Hexatungstate ***11f***. Yellow solid. IR (KBr, cm^{-1}): 3134.19 (C–H), 3042.55 (C–H), 976.17 (W=O), 785.60 (W–O–W). Anal. Calcd. For $C_{56}H_{68}Br_2N_4W_6O_{19}$ (2364.00): C, 28.45; H, 2.90; N, 2.37. Found: C, 28.41; H, 2.88; N, 2.39.

Hexamolybdate ***12a***. Orange yellow solid. IR (KBr, cm^{-1}): 3146.83 (C–H), 3109.36 (C–H), 943.21 (Mo=O), 892.37 (Mo–O–Mo). Anal. Calcd. For $C_{58}H_{44}Br_2N_4Mo_6O_{19}$ (1836.43): C, 37.93; H, 2.41; N, 3.05. Found: C, 37.91; H, 2.37; N, 3.07.

Hexamolybdate ***12b***. Orange yellow solid. IR (KBr, cm^{-1}): 3159.23 (C–H), 3091.41 (C–H), 955.25 (Mo=O), 889.56 (Mo–O–Mo). Anal. Calcd. For $C_{58}H_{42}Br_2F_2N_4Mo_6O_{19}$ (1872.41): C, 37.20; H, 2.26; N, 2.99. Found: C, 37.11; H, 2.23; N, 3.04.

Hexamolybdate ***12c***. Orange yellow solid. IR (KBr, cm^{-1}): 3153.15 (C–H), 3096.18 (C–H), 948.23 (Mo=O), 881.07 (Mo–O–Mo). Anal. Calcd. For $C_{58}H_{42}Br_2Cl_2N_4Mo_6O_{19}$ (1905.32): C, 36.56; H, 2.22; N, 2.94. Found: C, 36.47; H, 2.19; N, 3.01.

Hexamolybdate ***12d***. Orange yellow solid. IR (KBr, cm^{-1}): 3158.11 (C–H), 3097.44 (C–H), 941.60 (Mo=O), 892.75 (Mo–O–Mo). Anal. Calcd. For $C_{58}H_{42}Br_4N_4Mo_6O_{19}$ (1994.23): C, 34.93; H, 2.12; N, 2.81. Found: C, 34.88; H, 2.09; N, 2.84.

Hexamolybdate ***12e***. Orange yellow solid. IR (KBr, cm^{-1}): 3161.20 (C–H), 3091.28 (C–H), 945.28 (Mo=O), 898.10 (Mo–O–Mo). Anal. Calcd. For $C_{68}H_{64}Br_2N_4Mo_6O_{19}$ (1976.70): C, 41.32; H, 3.26; N, 2.83. Found: C, 41.25; H, 3.22; N, 2.89.

Hexatungstate ***13a***. Yellow solid. IR (KBr, cm^{-1}): 3139.85 (C–H), 3048.49 (C–H), 980.56 (W=O), 788.21 (W–O–W). Anal. Calcd. For $C_{58}H_{44}Br_2N_4W_6O_{19}$ (2363.83): C, 29.47; H, 1.88; N, 2.37. Found: C, 29.39; H, 1.86; N; 2.38.

Hexatungstate ***13b***. Yellow solid. IR (KBr, cm^{-1}): 3144.18 (C–H), 3040.13 (C–H), 981.67 (W=O), 792.63 (W–O–W). Anal. Calcd. For $C_{58}H_{42}Br_2F_2N_4W_6O_{19}$ (2399.81): C, 29.03; H, 1.76; N, 2.33. Found: C, 28.95; H, 1.71; N, 2.36.

Hexatungstate ***13c***. Yellow solid. IR (KBr, cm^{-1}): 3143.59 (C–H), 3049.97 (C–H), 976.23 (W=O), 792.14 (W–O–W). Anal. Calcd. For $C_{58}H_{42}Br_2Cl_2N_4W_6O_{19}$ (2432.72): C, 28.64; H, 1.74; N, 2.30. Found: C, 28.59; H, 1.72; N, 2.33.

Hexatungstate ***13d***. Yellow solid. IR (KBr, cm^{-1}): 3141.72 (C–H), 3036.36 (C–H), 979.30 (W=O), 790.85 (W–O–W). Anal. Calcd. For $C_{58}H_{42}Br_4N_4W_6O_{19}$ (2521.63): C, 27.63; H, 1.68; N, 2.22. Found: C, 27.58; H, 1.66; N, 2.25.

Hexatungstate ***13e***. Yellow solid. IR (KBr, cm^{-1}): 3137.54 (C–H), 3029.12 (C–H), 978.86 (W=O), 793.45 (W–O–W). Anal. Calcd. For $C_{68}H_{64}Br_2N_4W_6O_{19}$ (2504.10): C, 32.62; H, 2.58; N, 2.24. Found: C, 32.53; H, 2.55; N, 2.26.

A General Procedure for Obtaining Single Crystals, Suitable for Single Crystal X-ray Crystallography.

A small amount of the ion pair compound (30 mg), to be recrystallized, was dissolved in minimum amount of DMSO by sonication to prepare a saturated solution in a small vial. This open small vial was then placed into an another bigger vial containing diethyl ether and the bigger vial was then capped / closed so that diethyl ether diffused into DMSO solution of the ion pair compound. Single crystals, appeared during one week or so, were subjected to single crystal X-ray crystallography for data collection.

2.2. Crystal structure determination

Single-crystals suitable for structural determination of the compounds **10a**, **10d**, **11a**-**e**, **13a-e**, were mounted on a three circle Bruker SMARTAPEX CCD area detector system under Mo Kα (λ = 0.71073 Å) graphite monochromated X-ray beam with crystal-to-detector distance of 60 mm, and a collimator of 0.5 mm width. The scans were recorded with a ω scan width of 0.3°. Data reduction was performed by SAINTPLUS [31], empirical absorption corrections using equivalent reflections were performed by program SADABS [32]. Structure solutions were done using SHELXS-97 [33] and fullmatrix least-squares refinement was carried out using SHELXL- 97 [34] for all compounds. All the non-hydrogen atoms were refined anisotropically. Hydrogen atoms on the C atoms were introduced on calculated positions and were included in the refinement riding on their respective parent atoms. Crystal data and structure refinement parameters for the compounds are summarized in Tables 1-5.

3. Results and discussion

3.1. Synthesis

9–Anthracene methanol (**1**) has been used as the starting precursor to obtain the anthracene based cations. Treatment of one equivalent triphenyl phosphine with two equivalents of molecular bromine generates the Lewis acid–base adduct $PPh_3 \cdot Br_2$ that brominates the alcohol function of **1** whereas, the remaining free molecular bromine brominates the anthracene ring at the 9th position resulting in the formation of the desired brominated precursor 9–bromo–10–bromomethyl–anthracene (**2**) [9]. N–alkyl–imidazoles (**4a**–**f**) and N–benzyl–benzimidazoles (**7a**–**e**) have been synthesized from imidazole (**3**) and benzimidazole (**5**) respectively, by means of base mediated electrophillic substitution at nitrogen (see Scheme 3). All the reactions have been carried out in air in DMSO using NaOH as the base.

Choice over the solvent and base is arbitrary in the present study as any other solvents like THF, MeCN, toluene *etc*. or base like triethylamine, diisopropylamine, sodium hydride *etc*. can also be conveniently used for these reactions.

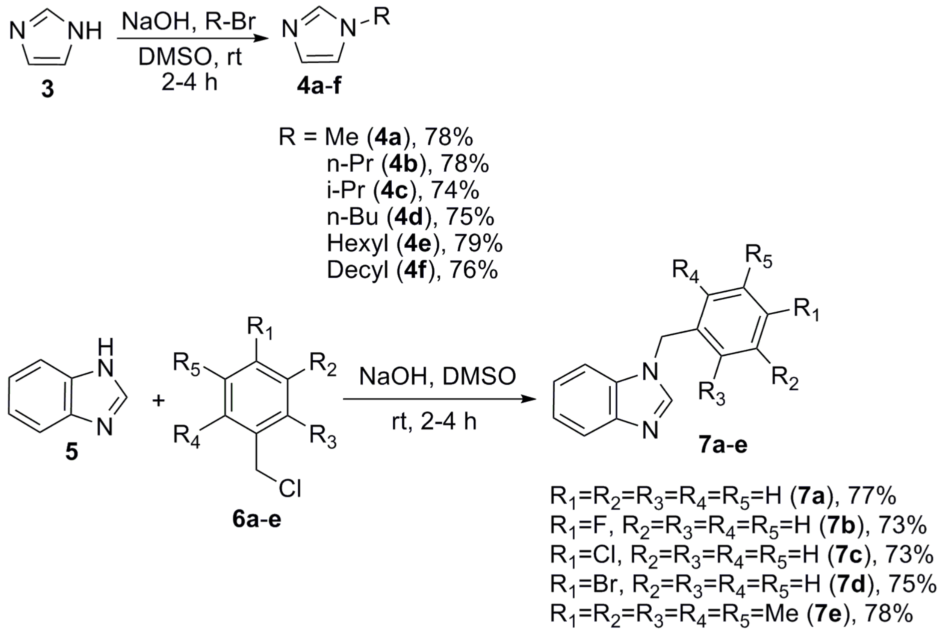

Scheme 3. Synthesis of the N–alkyl–imidazoles and N–benzyl–benzimidazoles.

Sometimes, usage of a phase transfer catalyst, for example, 18–crown–6, tetrabutylammonium bromide, benzenetriethylammonium chloride *etc*. help in smoother progress of such reactions. However, in the present case, no phase transfer catalyst has been used, as the monitoring of the reactions by TLC indicates clear progress of the same without any catalyst. Similarly, reaction conditions, such as, dry solvent or heat *etc*. have not explored any considerable improvement of the product yields, thereby the reactions were carried out in air at an ambient condition. Addition of 1.5 equiv. of base in a DMSO solution of **3** or **5**, followed by slow addition of the corresponding electrophiles (alkyl bromides or benzyl chlorides) at 20–25 ºC results in formation of the products (**4a**–**f** and/or **7a**–**3**, Scheme 3). They have been isolated in good yields after regular workups followed by purification through column chromatography (silica gel, 100–200 mesh, MeOH : EtOAc = 5:95 v/v, see experimental section). Purification of the N–alkyl imidazoles by distillation method has been avoided because of their high boiling points and chances of product loss due to decomposition at elevated temperature. All the isolated compounds have been characterized by NMR (^{1}H and ^{13}C) spectroscopy, LC–MS and successful elemental analysis.

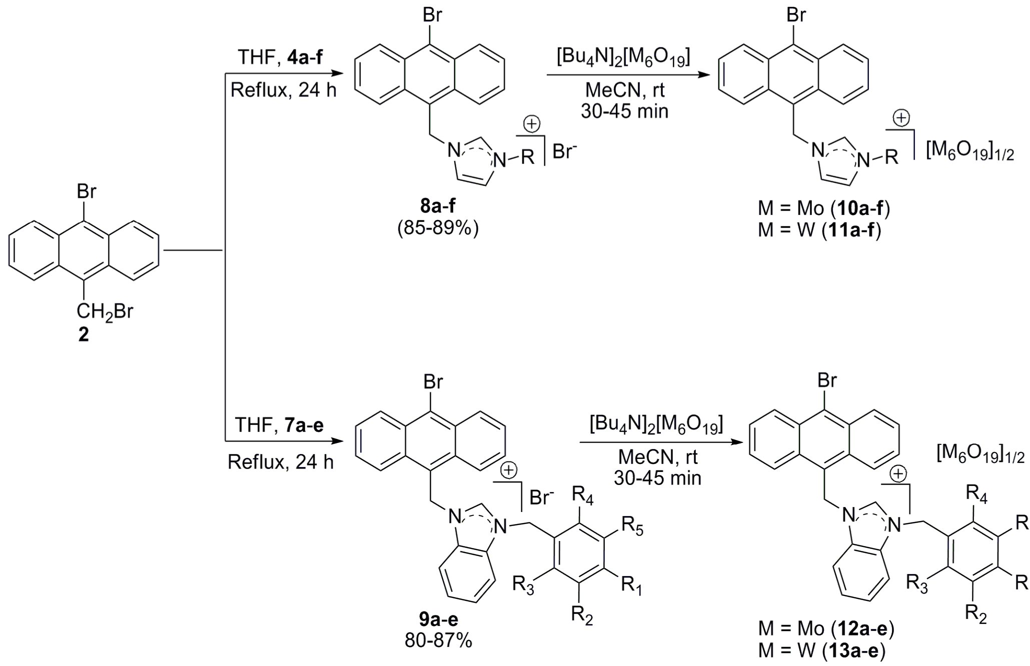

Scheme 4. Synthesis of the POM–anthracene ion–pair compounds.

Reactions between 9–bromo–10–(bromomethyl)anthracene (**2**) and the corresponding N–alkyl imidazoles (**4a**–**f**) / N–benzyl benzimidazoles (**7a**–**e**) in THF under refluxing condition have resulted in precipitation of the corresponding bromide salts **8a**–**f** and **9a**–**e** respectively (see Scheme 4), that have been isolated by filtration. Stoichiometric ion–exchange between these salts with $[Bu_4N]_2[M_6O_{19}]$ (2:1) (M = Mo, W) in acetonitrile renders immediate precipitation of the hexamolybdate or hexatungstate salts of the anthracene cations. Molybdate salts (**10a**–**f**, **12a**–**e**, Scheme 4) are orange in color while tungstates (**11a**–**f**, **13a**–**e**, Scheme 4) are yellow- colored. Single crystals, suitable for X–ray diffraction analysis, have been grown by diffusion of diethyl ether into DMSO solutions of the respective POM salts.

3.3. Description of Crystal structures

The hexametalate POM cluster anions have isometric (almost spherical) shape and the polyaromatic hydrocarbon anthracene is of highly anisometric (flat) shaped with π–electron clouds above and below the plane of the molecule. Therefore, to co-crystallize these structurally incompatible / mismatched molecular components (hexametalates and anthracene), sufficient energy should be provided to overcome the destabilization that arises due to presence of them in the same crystal lattice. In this regard, Coulombic forces have been shown to play the major role towards the stabilization of the co-crystals, thus built from the structurally mismatched components.[27] Basically one cationic fragment should be attached with the anthracene ring to associate the cation with the POM surface through electrostatic / Coulombic forces and the anthracene ring, if possible, would orient itself to the POM surface. Thus, in the present case, N–alkyl imidazolium or N–benzyl benzimidazolium moieties have been used as the cationic anchors to the anthracene–based cations. The cationic counterparts in all the cases are attached to the anthracene ring *via* a methylene spacer (–CH_2–). Although the solids (**10a**–**13e**, Scheme 4), obtained by the ionic metathesis between the POM cluster anions (tetrabutylammonium salt) and anthracene–based cations (bromide), can best be considered as salts or ion–pair solids, we would like to use the phrase '**Coulombic co-crystals**' to describe them. The reason, we have used this term, is the Coulombic forces that contribute towards the stabilization of such isometric : anisometric cocrystals (**10a**–**13e**, Scheme 4). X-ray diffraction quality crystals have been grown using ether as the anti-solvent (precipitant) to the DMSO solutions of the respective solids.

Molecular structures of the crystallographically characterized solids have been presented in Figures 1–2. Mainly the tungstate salts have been structurally characterized. For the comparison purpose, two molybdates (**10a** and **10d**) have been crystallographically characterized. Crystals of molybdate- and tungstate-salts of the same countercation are found to be isomorphous / isostructural, as observed from unit cell parameters of the compounds **10a** and **11a** (or **10d** and **11d**), that are almost identical, thereby making the molecules in the concerned solids pack under same space symmetry. Thus, changing the metal centers of the Lindqvist type isopolyanions from molybdenum to tungsten has not induced any significant alteration of the molecular ensemble. This is clearly in accord with the expectation as both the $[Mo_6O_{19}]^{2-}$ and $[W_6O_{19}]^{2-}$ cluster anions have many similar features e.g. almost spherical shape, octahedral symmetrical (O_h) *etc.* The crystal structures of ion pair compounds **13a**–**e** are presented in Figure 3.

All crystal structures consist of two cations and one POM cluster anion. Some of the crystals have been isolated as DMSO solvates. Structural analysis of the relevant solids reveals some common features, which are summarized below.

(a) Asymmetric units of all the crystal structures consist of one anthracene–based mono–cation and half of the POM cluster di–anion for electro-neutrality. All the molecules are centrosymmetric with respect to the centre of inversion at the central oxygen atom of the POM cluster anions. The full molecules are generated upon operation of the inversion symmetry on the concerned asymmetric units. Therefore, the title solids have maintained 2:1 stoichiometry between the cations and the anions and the respective solids are considered as stoichiometric solids.

(b) The imidazolium / benzimidazolium cationic counterparts in all the structures have been observed to face toward one of the octrahedral facets of the POM cluster anions due to Coulombic association between them.

(c) The anthracene rings are away of the POM surfaces and pack with each other through $\pi\cdots\pi$ stacking interactions. No $\pi\cdots$POM interactions are observed in the relevant crystals where the π–stacked anthracenes interact with the POM cluster anions only by C–H$\cdots$O weak hydrogen bonding interactions. Thus, the solids described in this article cannot be considered as donor–acceptor $\pi\cdots$POM solids even though they are intensely colored contrast to their starting precursors in their solid states.

Two different space symmetry *viz. P–1* (triclinic) and $P2_1/c$ (monoclinic) have been observed for the crystal packing of the compounds containing anthracene–imidazolium counter cations (**10a**–**11f**). The crystals, containing methyl, i–propyl, hexyl and decyl alkyl chains in the imidazolium cationic counterparts, feature packing of the molecules obeying the lower space symmetry (*P–1*). But, in case of the *n*–propyl and butyl alkyl chains, the molecules tend to crystallize under higher special symmetry ($P2_1/c$). This symmetry alteration might be due to variation of the hydrogen boding environments in the relevant solids. In all the cases, molecules have crystallized with one cation and half of the POM cluster anion in the asymmetric unit (Z' = ½). In the symmetric unit, the two cations are related to each other by the inversion symmetry with respect to the central oxygen atom of the cluster anion. Although the structural analysis of the solids **11a**–**f** exhibit many similarities in packing of the molecules, a little change in the intermolecular interactions has been observed with the variation of the alkyl chain lengths in the cations. The imidazolium ring has a rotational freedom around the C(15)–N(1) bond and this rotation determines the dihedral angle between the anthracene and imidazolium planes. Variation of the alkyl chain lengths in the imidazolium cations causes a change in this torsion angle in an irregular manner. There is a partial overlapping between the anthracene rings in the relevant crystals as shown in Figure 4. In the crystal structures of the compounds **10a**, **11c** and **11e**, the imidazolium and anthracene planes are oriented in such an angular span, that interactions between two inversion symmetry related cations result in the formation of a π–stacked dimer (**10a**, **11c** and **11e**, Figure 4). The crystals of other compounds of Figure 4 exclude such dimer formation due to improper spatial orientation of the imidazole and the anthracene rings, although there is C–H$\cdots\pi$ stacking interactions between the alkyl chain of one cation with the anthracene ring of the other inversion related cation. No direct interaction between the π–cloud of the anthracene ring and the POM surface is noticed in these solids. Thus, the lattice energy of such Coulombic cocrystals incorporating both flat and spherical shaped molecular components are minimized by the abundance of Coulombic association between the imidazolium cations and POM anions, C–H···O weak hydrogen bonding interactions with the POM acceptors, C–H···π and π···π stacking interactions between the various crystal components.

In all these solids, the anthracene cations have packed with each other through π···π stacking interactions in a *trans*–fashion as far as orientations of the N–alkyl imidazolium moieties and bromine atoms are concerned. A little change in the distance between centroids of two such stacked anthracene rings has been observed with the variation of the alkyl chain. These π–stacked anthracene rings have further interacted with the POM anions through C–H···O supramolecular interactions in an alike fashion as mentioned in Scheme 1a.

Rotational freedom of C–C bond around the benzimidazolium plane in 13a-13e

The crystal structures, discussed so far, contain only one π–ring i.e. the anthracene ring attached to the imidazolium moiety. The situation is bit different in the case of N–benzyl benzimidazolium cations which consist of more number of π–rings. The imidazolium cation consists only one π–ring-system, i.e. the anthracene ring but the benzimidazolium cations comprise of three π–rings *viz.* the anthracene ring, benzimidazole ring and the phenyl ring of the benzyl counterpart. Both the anthracene and the benzene ring of the benzyl fragment have C–C rotational freedom around the benzimidazolium plane (Table 6). Thus, these cations are more puckred compared to the alkylimidazolium cations. The only structural difference between the benzimidazolium cations is the variation of bulkiness in the benzyl group. As previously stated, PXRD analysis of the molydates and the tungstates have revealed isostructurality between the two, only the tungstate analogous (**13a**–**e**) have been crystallographically characterized. The solid **12a** and **13a** do not contain any substitution on the benzyl ring whereas, in case of the others, bulkiness of the benzyl groups has been increased by attaching F (**12b**, **13b**), Cl (**12c**, **13c**), Br (**12d**, **13d**) and five methyl groups (**12e**, **13e**). Depending upon the spatial spans of the anthracene and the phenyl (benzyl) rings, the cations can be classified into three rotamers *i.e. eclipsed*, *gauche* and *staggered* as shown in Table 6. If both of them are projected at the same side of the benzimidazolium plane, the conformation of the concerned cation is *eclipsed*. Similarly, if the relevant C–C rotations make them to flang on opposite direction of the mentioned plane, then the conformation of the cation is *staggered*. For the *gauche* conformation, both the rings are on the same direction of the benzimidazolium plane, but at a certain dihedral angle between 0 and 180º. Crystal structures of the solids **13a**–**e** have been presented in Figure 3.

As shown in Figure 3, structures of all the compounds **13a**–**e** are characterized by one cation and half of the POM cluster anion in the asymmetric unit (Z' = ½). In the relevant crystals, two different orientations of the anthracene and the phenyl (benzyl) rings have been observed with respect to the benzimidazolium plane. Several observed angular parameters in the concerned crystal structures have been summarized in Table 6. Crystallographically observed angular spans of the anthracene and the phenyl ring of the benzyl fragment have been pictorially represented in Figure 5 that clearly depicts *eclipsed* and *gauche* orientations of the concerned rings in the relevant crystals. However, alike all the crystals built from N–alkyl imidazolium cations, the present case also demonstrate similar crystal packing features and will not be discussed separately. For example, in all the crystals (**13a**–**e**), the anthracene rings are stacked with each other *via* π···π stacking interactions, the benzimidazolium cationic counterparts are oriented toward a facet of the POM anions due to Coulombic association and the cations are further associated with the POM cluster anions *via* supramolecular C–H···O hydrogen bonding interactions. Two representative crystal–packing features have been displayed in Figure 6. Due to more bulkiness of the benzyl benzimidazolium cations compared to the alkyl imidazolium cations, complete overlap between the π–electron clouds of two anthracene rings have been forbidden and a partial overlapping between the two rings have been observed in the relevant crystals. Thus, changing the cation from alkyl imidazolium to benzyl benzimidazolium has not induced much difference in the packing feature of the molecules in their respective crystals.

Spectroscopy

It has already been mentioned that, the hexamolybdate ($[Mo_6O_{19}]^{2-}$) salts are intense orange–red and the hexatungstate ($[W_6O_{19}]^{2-}$) salts are intense yellow in color in their solid states. Dissolution of the molybdates in DMF or in DMSO (these salts are not soluble in other common organic solvents e.g. MeCN, MeOH etc.) causes disappearance of the orange-red color and a pale yellow color persists in the solution. Absorption spectra of the resulting solutions are found to be equivalent to that obtained from a 2:1 physical mixture of the anthracene cations and $[Bu_4N]_2[Mo_6O_{19}]$. Even the absorption properties of the solutions remain invariant upon addition of large amount of the ionic counterparts. The corresponding absorption spectra are characterized by discrete and broad absorptions due to the anthracene cations and the hexamolybdate cluster anion in solution. The similar matter is observed for the hexatungstate analogues. Contrast to the solution–state absorption spectra of the concerned solids, the solid–state absorption spectra show remarkable difference. Absorption spectra of the concerned solids have been obtained by the diffused reflectance technique by dispersing the powdery samples in $BaSO_4$. Both the various anthracene cations (**8a-f** and **9a-e**), $[Bu_4N]_2[Mo_6O_{19}]$ and $[Bu_4N]_2[W_6O_{19}]$ are transparent (solid–state) at wavelengths more than 500 nm. The $[Bu_4N]_2[W_6O_{19}]$ cluster absorb at higher energy ($\lambda_{max} < 300$ nm) than the $[Bu_4N]_2[Mo_6O_{19}]$ cluster ($\lambda_{max} \approx 345$ nm). Both of the cluster precursors exhibit structureless absorption patterns. A structured broad absorption band ($\lambda_{max} \approx 380$ nm) features the solid–state absorption spectra of the anthracene cations as shown in Figure 7. Also, the 2:1 physical mixtures of the anthracene bromide salts and the POM tetrabutylammonium salts exhibit the similar feature. The concerned ion–exchanged molybdates, described in this article, rather feature a modulated absorption spectra *i.e.* appearance of a new band (or tail) in the visible region of the spectra ($\lambda > 500$ nm). The yellow tungstates exhibit a tail initiating from *ca.* 550 nm. Again, in all the cases, the absorption spectra of the anthracene–POM salts exhibit very distinct features than the same of their ionic parents. For example, the absorption bands due to the hexametalate cluster anions and anthracene remain indistinctive in the absorption spectra of the anthracene–POM solids demonstrated here. Therefore, commencement of the new bands in the visible region is due to some sort of interaction between the molecular components only in the solid state. In another words, it can be said that spectroscopic identities of the anthracene and hexametalate counterparts vanish upon their ionic and supramolecular association in the solid state and results in an intense color of the resulting ion pair compounds in their solid states. This intense color of the ion pair compounds in their solid state is probably due to the broad shoulder-like feature in the region of 450-550 nm in their diffuse reflectance spectra (Figure 7). We assign this feature as solid state intra-ion-pair transition.

4. Conclusion

Surprisingly, crystallographic analyses on the present synthesized solids (**10a**–**11f**, **12a**–**13e**) have not revealed any $\pi\cdots$POM interaction between anthracene and the POM cluster anions. Single crystal- as well as powder X–ray diffraction analyses show that both the molybdate and tungstate salts of the same counter cation are isostructural.

In conclusion, a series of hexametalate cluster based solids comprising of various anthracene-imidazolium and anthracene-benzimidazolium cationic counterparts have been synthesized and their structures have been determined through crystallography. Both the hexamolybdates and hexatungstates of the same counter cation are isomorphous. All the solids maintain 2:1 stoichiometry between the mono-cations and the di-anions and are centrosymmetric with respect to the central oxygen atom of the octahedral symmetrical POMs. The cationic counterparts (imidazolium and benzimidazolium) in all the solids project toward surface of the POMs due to electrostatic interaction between the oppositely charged species. Apart from coulombic association between the anthracenes and the POM, supramolecular hydrogen bonding interactions are also observed to optimize the lattice destabilization due to coexistence of the structurally mismatched molecular components in the same crystal. Color of the molybdates are observed only in the solid state and probably no adduct formation takes place in the solution state as revealed by the solid state as well as the solution state UV-visible spectroscopy. Variation of the alkyl chain lengths in the imidazolium cationic moiety or alteration of the substituent in the benzimidazolium moiety does not change the intermolecular association of the components to a greater extent. Possibly, due the shorter spacer, the anthracene ring could not interact with the POM surface, which results in charge transfer interaction between the two. In the solid state, the title compounds show an intense color (that is absent in both of their constituents, cations and anions), which has been assigned to a solid state intra-ion-pair transition.

Acknowledgements

We thank SERB, Department of Science and Technology (DST), Government of India, for financial support (Project No. SB/S1/IC-34/2013). We also thank UPE-II (UGC) for some financial support.

Appendix A. Supplementary data

CCDC 1514215, CCDC 1514216 and CCDC 1514231 contain the supplementary crystallographic data for compounds **10a**, **11a** and **10d** respectively. CCDC 1514232 – CCDC 1514241 contain the supplementary crystallographic data for compounds **11b-f** and **13a-e** respectively. Relevant crystal data can be obtained free of charge via http://www.ccdc.cam.atc.uk/conts/retrieving.html, or from the Cambridge Crystallographic Data Centre, 12 Union Road, Cambridge CB2 1EZ, UK; fax: (+44) 1223−336− 033; or e-mail: deposit@ccdc.cam.ac.uk.

References

[1] (a) G. P. Stahly, Cryst. Growth Des. 7 (2007) 1007-1026.
  (b) J. D. Dunitz, CrystEngComm 4 (2003) 506-506.
  (c) G. R. Desiraju, CrystEngComm 5 (2003) 466-467.
  (d) A. D. Bond, CrystEngComm 9 (2007) 833-834.

[2](a) A. I. Kitaigorodsky, Mixed Crystals Springer–Verlag: Berlin, 1984.
  (b) A. B. Aakeröy, D. J. Salmon, CrystEngComm 7 (2005) 439-448.
  (c) P. Vishweshwar, J. A. McMahon, M. J. Zaworotko, J. Pharm. Sci. 95 (2006) 499-516.
  (d) W. Jones, W. D. Motherwell, A. V. Trask, MRS Bull. 341 (2006) 875-879.
  (e) S. L.Childs, K. I. Hardcastle, Cryst. Growth Des. 7 (2007) 1291-1304.
  (f) A. B. Bond, CrystEngComm 9 (2007) 833.
  (g) B. R. Bhogala, A. Nangia, New J. Chem. 32 (2008) 800-807.

[3] G. P. Stahly, Cryst. Growth Des. 9 (2009) 4212-4229 and the references therein.

[4] F. Wohler, Annalen Chem. Pharm. 51 (1844) 145-163.

[5] J. S. Anderson, Nature 14 (1937) 850-850.

[6] For a review see: N. Schultheiss, A. Newman, Cryst. Growth. Des. 9 (2009) 2950-2967 and the references therein.

[7] N. G. Anderson, D.A. Lust, K. A. Colapret, J. H. Simpson, M. F. Malley, J. Z. Gougoutas, J. Org. Chem. 61 (1996) 7955-7958.

[8](a) P. M. Bhatt, N. V. Ravindra, R. Banerjee, G. R. Desiraju, Chem. Commun. 2005, 1073-1075.
  (b) S. Biswas, R. Saha, I. M. Steele, S. Kumar, K. Dey, J. Chem. Crystallography 43 (2013) 493-501.
  (c) C. B. Aakeroy, D. Welideniya, J. Desper, C. Moore, Cryst.Eng.Comm. 16 (2014) 10203-10209.
  (d) K. A. Powell, G. Bartolini, E. Wittering, A. N. Saleemi, C. C.Wilson, C. D. Rielly, Z. K. Nagi, Cryst. Growth Des. 15 (2015) 4821-4836.
  (e) X. Zhang, Y. Tian, J. Jio, T. Zhang, G. Zhu, J. Mol. Struct. 1108 (2016) 560-566.
  (f) N. I. Nadzri, N. H. Sabri, V. S. Lee, H. Abdul, N. Siti, J. Chem. Crystallography 46 (2016) 144-154.
  (g) A. Cvetkovski, V. Bertolasi, V. Ferreti, Acta Cryst., Sec. B: Struct. Science, Cryst. Engg. And Materials 72 (2016) 320-324.

(h) C. Wood, A. Alwati, S. Halsey, T. Gough, E. Brown, A. Kelly, A. Porakar, J. Pharma. Biomed. Anal. 129 (2016) 172-181.

(i) C. Pando, A. Cabonas, I. A. Cuadra, RSC Adv. 6 (2016) 71134-71150.

(j) I. Sovago, W. Wang, D. Qiu, D. Raijada, J. Rantanen, H. Grobganz, T. Rades, A. D. Bond, K. Loebmann, K. Molecules 21 (2016) 509/1-13.

[9](a) J. M. Lehn, Supramolecular chemistry: concepts and perspectives Wiley–VCH, (1995).

(b) G. R. Desiraju, Supramol. Chem. 6 (1996) 1-22

(c) A. Anthony, G. R. Desiraju, R. K. R. Jelti, S. S. Kudva, N. N. L. Madhavi, A. Nangia, R. Thaimattam, V. R. Thalladi, Cryst. Engg. 1 (1998) 1-18.

(d) J. W. Steed, J. L. Atwood, Supramolecular Chemistry John Wiley and Sons, (2009).

(e) J. W. Steed, J. L. Atwood, M. Dekker, Encyclopedia of Supramolecular Chemistry Vol. 2, (2004).

(f) A. Nangia, J. Chem. Sc., 122 (2010) 295-310

[10] M. M. Olmstead, A. K. Maitra, A. L. Balch, Angew. Chem., Int. Ed. 38 (1999) 231-233.

[11](a) J. L. Atwood, L. J. Barbour, C. L. Raston, I. B. N. Sudria, Angew.Chem., Int. Ed. 37 (1998) 981-983.

(b) J. L. Atwood, G. A. Koutsantonis, C. L. Raston, Nature 368 (1994) 229-231.

(c) D, E. Cliffel, A. J. Bard, S. Shinkai, Anal. Chem. 70 (1998) 4146-4151.

(d) T. Suzuki, K. Nakashima, S. Shinkai, Tetrahedron Lett. 36 (1995) 249-252.

(e) A. Drijaca, C. Kepert, L. Spiccia, C. L. Raston, C. A. Sandoval, T. D. Smith, Chem. Commun. (1997), 195-196.

(f) T. Haino, M. Yanase, Y. Fukazawa, Angew. Chem., Int. Ed. 37 (1998) 997-998.

(g) K. Tsubaki, K. Tanaka, T. Kinoshita, K. Fuji, Chem. Commun. (1998) 895-896.

(h) R. M. Williams, J. M. Zwier, J. W. Verhoeven, J. Am. Chem. Soc. 116 (1994) 6965-6966.

(i) L. J. Barbour, G. W. Orr, J. L. Atwood, Chem. Commun. (1997) 1439-1440.

(j) L. J. Barbour, G. W. Orr, J. L. Atwood, Chem. Commun. (1998) 1901-1902.

(k) P. J. Nichols, C. L. Raston, C. A. Sandoval, D. J. Young, Chem.Commun. (1997) 1839-1840.

(l) T. Haino, M. Yanase, Y. Fukazawa, Angew. Chem., Int. Ed. 36 (1997) 259-260.

(m) B. Paci, G. Amoretti, G. Arduini, G. Ruani, S. Shinkai, T. Suzuki, F. Ugozzoli, R. Caciuffo, Phys. Rev. B 53 (1997) 5566-5569.

[12](a) Z. Yoshida, H. Takekuma, S. Takekuma, Y. Matsubara, Angew.Chem., Int. Ed. 33

(1994) 1597-1599.

(b) T. Andersson, G. Westman, G. Stenhagen, M. Sundahl, O. Wennerström, Tetrahedron Lett. 36 (1995) 597-602.

[13](a) R. S. Burkhalter, J. Am. Chem. Soc. 116 (1994) 10346-10347.

(b) J. L. Atwood, M. Barnes, M. G. Gardiner, C. L. Raston, Chem. Commun. (1996) 1449-1450.

[14]P. C. Andrews, J. L. Atwood, L. J. Barbour, P. J. Nichols, C. L. Raston, Chem. Eur. J. 4 (1998) 1384.

[15](a) A. Ikeda, C. Fukuhara, S. Shinkai, Chem. Lett. (1997) 407.

(b) T. Drovetskaya, C. A. Reed, P. D. W. Boyd, Tetrahedron Lett. 36 (1995) 7971-7975.

(c) H. Imahori, K. Hagiwara, T. Akiyama, S. Taniguchi, T. Okada, S. Sakata, Chem. Lett. (1995), 265.

(d) H. Imahori, Y. Sakata, Chem. Lett. (1996), 199.

(e) T. Akiyama, H. Imahori, A. Ajawakom, Y. Sakata, Chem. Lett. (1996), 907.

(f) P. A. Liddell, D. Kuciauskas, J. P. Sumida, B. Nash, D. Nguyen, A. L. Moore, D. Gust, J. Am. Chem. Soc. 119 (1997) 1400-1405.

(g) H. Imahori, K. Yamada, M. Hasegawa, S. Taniguchi, T. Okada, Y. Sakata, Y. Angew.Chem., Int. Ed. 36 (1997) 2626-2629.

(h) H. Imahori, Y. Sakata. Adv. Mater. 9 (1997) 537-546.

(i) D. Kuciauskas, S. Lin, G. R. Seely, A. L. Moore, D. Gust, T. Drovetskaya, C. A. Reed, P. D. W. Boyd, J. Phys. Chem. 100 (1996) 15926-15932.

(j) Y. Sun, T. Drovetskaya, R. D. Bolskar, R. Bau, P. D. W. Boyd, C. A. Reed, J. Org. Chem. 62 (1997) 3642-3649.

(k) E. Dietel, A. Hirsch, E. Eichhorn, A. Rieker, S. Hackbarth, B. Röder, Chem. Commun. (1998) 1981-1982.

[16](a) M. M. Olmstead, D. A. Costa, K. Maitra, B. C. Noll, S. L. Phillips, P. M. Van Calcar, A. L. Balch, J. Am. Chem. Soc. 121 (1999) 7090-7097.

(b) P. D. W. Boyd, M. C. Hodgson, C. E. F. Rickard, A. G. Oliver, L. Chaker, P. J. Brothers, R. Bolskar, F. S. Tham, C. A. Reed, J. Am. Chem. Soc. 121 (1999) 10487-10495.

(c) T. Ishii, N. Aizawa, M. Yamashita, H. Matsuzaka, T. Kodama, K. Kikuchi, I. Ikemoto, Y. Iwasa, J. Chem. Soc., Dalton Trans. (2000) 4407-4412.

[17] M. T. Pope, Heteropoly and Isopoly Oxometalates Springer–Verlag: Berlin, (1983).

[18](a) A. Müller, E. Beckmann, H. Bögge, M. Schidtmann, A. Dress, Angew. Chem. Int.

Ed. 41 (2002) 1162-1167.

(b) P. J. Kulesza, L. R. Faulkner, Proc. Electrochem. Soc. 94 (1994) 20.

(c) T. Yamase, Kikan Kagaku Sosetsu. 20 (1993) 190.

(d) T. Sanac, K. Akira, H. Koichiro, K. Tetsuichi, Solid State Ionics 70-71 (1994) 636.

(e) K. Nomiya, M. Miwa, Polyhedron 4 (1985) 675-679.

(f) K. Nomiya, Polyhrdron 6 (1987) 309-314.

(g) K. Nomiya, M. Miwa, Polyhedron 3 (1984) 341-346.

(h) A. Müller, S. K. Das, C. Kuhlmann, H. Bögge, M. Schidtmann, E. Diemann, E. Krickmeyer, J. Hormes, H. Modrow, M. Schindler, Chem. Commun. (2001) 655-656.

(i) A. Müller, R. Maiti, M. Schidtmann, H. Bögge, S. K. Das, W. Zhang, Chem. Commun. (2001) 2126-2127.

(j) W. Yang, C. Lu, Lin, X. H. Zhuang, Chem. Commun. (2000) 1623-1624.

(k) Z. Han, Y. Zhao, J. Peng, Y. Feng, J. Yin, Q. Liu, Electroanalysis 17 (2005) 1097-1102.

(l) A. Nicoara, A. Patrut, D. Margineanu, A. Müller, Electrochemistry Communications 5 (2003) 511-518.

(m) M. Sadakane, E. Steckhan, Chem. Rev. 98 (1998) 219-238 and the references therein.

[19] (a) S. S. Mal, B. S. Bassil, M. Ibrahim, S. Nellutla, J. van Tol, N. S. Dalal, J. A. Fernández, X. López, J. M. Poblet, R. N. Biboum, B. Keita, U. Kortz, Inorg. Chem. 48 (2009) 11636-11645.

(b) V. Ball, F. Bernsmann, S. Werner, J. C. Voegel, L. F. Piedra–Garza, U. Kortz, U. Eur. J. Inorg. Chem. (2009) 5115-5124.

(c) S. S. Mal, N. H. Nsouli, M. Carraro, A. Sartorel, G. Scorrano, H. Oelrich, L. Walder, M. Bonchio, U. Kortz, Inorg. Chem. 49 (2010) 7-9.

(d) Y. Y. Bao, L. H. Bi, L-X. Wu, S. S. Mal, U. Kortz, Langmuir 25 (2009) 13000-13006.

[20] (a) J. L. Stark, V. G. Jr. Young, E. A. Matta, Angew. Chem., Int. Ed. 34 (1995) 2547-2548.

(b) P. Gouzerh, A. Proust, Chem. Rev. 98 (1998) 77-112.

(c) I. Barnahum, H. Cohen, R. Neumann, Inorg. Chem. 42 (2003) 3677-3684.

(d) J. B. Strong, G. P. A. Yap, R. Ostrander, L. M. Liable–Sands, E. A. Matta, J. Am. Chem. Soc. 122 (2000) 3275-3277.

(e) W. Clegg, R. J. Errington, K. A. Fraser, S. A. Holmes, A. Schäffer, J. Chem. Soc., Chem. Commun. (1995) 455-456.

(f) J. B. Strong, B. S. Haggerty, A. L. Rheingold, E. A. Maatta, E. A. Chem. Commun. (1997) 1137-1138.

(g) J. B. Strong, G. P. A. Yap, R. Ostrander, L. M. Liable–Sands, A. L. Rheingold, R. Thouvenot, P. Gouzerh, E. A. Maatta, J. Am. Chem. Soc. 122 (2000) 639-649.

(h) Y. Wei, B. Xu, C. L. Barnes, Z. Peng, J. Am. Chem. Soc. 123 (2001) 4083-4084.

(i) Y. Wei, M. Lu, C.F.-C. Cheung, C. L. Barnes, Z. Peng, Inorg. Chem. 40 (2001) 5489-5490.

(j) J. L. Stark, A. L. Rheingold, E.A. Maatta, J. Chem. Soc., Chem. Commun. (1995) 1165-1166.

(k) J. Kang, J. A. Nelson, M. Lu, B. Xie, Z. Peng, D. R. Powell, Inorg. Chem. 43 (2004) 6408-6413.

(l) J. Kang, B. Xu, Z. Peng, X. Zhu, Y. Wei, D. R. Powell, Angew. Chem., Int. Ed. 44 (2005) 6902-6905.

(m) A. Müller, E. Krickemeyer, H. Bögge, Angew. Chem., Int. Ed. Engl. 37 (1998) 3359-3363

[21] (a) S. Roy, CrystEngComm. 16 (2014) 4667-4676;

(b) S. Das, S. Biswas, T. Balaraju, S. Barman, R. Pochamoni, S. Roy, J. Mater. Chem. A 4 (2016) 8875-8887.

[22] (a) M. Dabbabi, M. Boyer, J. P. Launay, Y. Jeannin, Electroanal. Chem. 76 (1977) 153-164.

(b) M. T. Pope, J. M. Varga, Inorg. Chem. 5 (1966) 1249-1254.

(c) J. P. Launay, J. Inorg. Nucl. Chem. 18 (1976) 807-809.

[23] For example see: V. Shivaiah, S. K. Das, Inorg. Chem. 44 (2005) 8846-8854.

[24] (a) T. Chatterjee, M. Sarma, S. K. Das, Cryst. Growth Des. 10 (2010) 3149-3163.

(b) T. Chatterjee, M. Sarma, S. K. Das, J. Mol. Struct. 981 (2010) 34-39.

(c) M. Sarma, T. Chatterjee, S. K. Das, Inorg. Chem. Commun. 13 (2010) 1114-1117.

(d) T. Akutagawa, D. Endo, H. Imai, S. Noro, L. Cronin, T. Nakamura, Inorg. Chem. 45 (2006) 8628-8637.

(e) J. Xiong, K. Kubo, S. Noro, T. Akutagawa, T. Nakamura, T. Cryst. Growth Des. 16 (2016) 800-807.

[25] See for example: (a) Y. Li, Na Hao; E. Wang, M. Yuan, C. Hu, N. Hu, H. Jia, Inorg. Chem. 42 (2003) 2729.

(b) W. You, E. Wang, Y. Xu, Y. Li, L. Xu, C. Hu, Inorg. Chem. 40 (2001) 5468.

(c) Y. Li, E. Wang, S. Wang, Y. Lu, C. Hu, N. Hu, H. Jia, J. Mol. Struct. 607 (2002) 133-141.

(d) X. Lu, B. Liu, Sarula, J. Wang, C. Ye, Polyhedron 24 (2005) 2889-2892.

(e) V. Shivaiah, Inorg. Chem. Commun. 9 (2006) 1191-1194.

(f) T. Akugatawa, D. Endo, F. Kudo, S. Noro, S. Takida, L. Cronin, T. Nakamura, T. Cryst. Growth Des. 8 (2008) 812-816.

(g) W. You, E. Wang, Q. He, L. Xu, Y. Xing, H. Jio, H. J. Mol. Struct. 524 (2000) 133-139.

(h) W. You, E. Wang, L. Xu, Z. Zhu, Y. Gu, J. Mol. Struct. 605 (2002) 41-49.

(i) Q. Du, D. Song, W. You, Y. Zhao, T. Gan, L. Z. Dai, Naturforsch. 64b (2009) 274-280.

[26] (a) J. Thomas, A. Ramanan, Cryst. Growth Des. 8 (2008) 3390-3400.

(b) K. Pavani, S. E. Lofland, K. V. Ramanujachary, A. Ramanan, Eur. J. Inorg. Chem. (2007) 568-578.

(c) S. Upreti, A. Ramanan, Crystal Growth Des. 6 (2006) 2066-2071.

(d) S. Upreti, A. Ramanan, Crystal Growth Des. 5 (2005) 1837-1843.

(e) K. Pavani, A. Ramanan, Eur. J. Inorg. Chem. (2005) 3080-3087.

(f) M. Asnani, S. Sharma, S. E. Lofland, K. V. Ramanujachary, P. A. Buffat, A. Ramanan, Eur. J. Inorg. Chem. (2005) 401-409.

(g) S. Chakrabarti, S. Natarajan, Crystal Growth Des. 2 (2002) 333-339.

[27] P. Le Maguere`s, S. M. Hubig, S. V. Lindeman, P. Veya, J. K. Kochi, J. Am. Chem. Soc. 122 2000) 10073-10082.

[28] C. Tan, W. Bu, J. solid State Chem. 219 (2014) 93-98.

[29] (a) S. H. Yang, O. J. Shon, K. M. Park, S. S. Lee, H. J. Park, M. J. Kim, J. H. Lee, J. S. Kim, Bull. Korean Chem. Soc. 23 (2002) 1585-1588.

(b) S. Duan, J. Turk, J. Speigle, J. Corbin, J. Masnovi, R. J. Baker, J. Org. Chem. 65 (2000) 3005-3009.

(c) M. Michelswirth, M. Rakers, C. Schafer, J. Mattay, M. Neumann, U. Heinzmann, J. Phys. Chem. B 114 (2010) 3482-3487.

(d) J. H. Clements, S. E. Webber, J. Phys. Chem. B 103 (1999) 9366.

(e) J. H. Clements, S. E. Webber, Macromolecules 37 (2004) 1531-1536.

[30] For spectroscopic data of the N–alkylimidazoles see: S. Khabnadideh, Z. Rezaei, A. Khalafi–Nezhad, R. Bahrinajafi, R. Mohamadia, A. A. Farrokhroza, Bioorg. Med. Chem. Lett. 13 (2003) 2863-2865.

[31] SAINT: Software for the CCD Detector System; Bruker Analytical X-ray Systems, Inc.:

Madison, WI, (1998).

[32] Sheldrick, G. M. SADABS: Program for Absorption Correction; University of Göttingen: Göttingen, Germany, (1997).

[33] Sheldrick, G. M. SHELXS-97: Program for Structure Solution; University of Göttingen: Göttingen, Germany, (1997).

[34] Sheldrick, G. M. SHELXL-97: Program for Crystal Structure Analysis; University of Göttingen: Göttingen, Germany, (1997)

Table 1 Crystal data and structure refinement parameters for compounds **10a** and **10d**

	10a	**10d**
Empirical formula	$C_{42}H_{44}Br_2Mo_6N_4O_{21}S_2$	$C_{48}H_{55}Br_2Mo_6N_4O_{21}S_2$
Formula weight	1740.39	1824.55
T (K), λ (Å)	298(2), 0.71073	298(2), 0.71073
Crystal system	triclinic	monoclinic
Space group	*P-1*	*P21/c*
a(Å)	10.705(5)	11.0467(7)
b(Å)	11.509(5)	12.3811(8)
c(Å)	12.013(6)	22.1829(14)
$\alpha(^O)$	116.856(6)	90.00
$\beta(^O)$	99.2150(10)	99.2150(10)
$\gamma(^O)$	90.529(7)	90.00
V(Å^3)	1317.1(10)	2994.8(3)
Z, d_{calcd}(g cm^{-3})	1, 2.194	2, 2.023
μ(mm^{-1}), F(000)	3.062, 846	2.699, 1788
GooF on F^2	1.059	1.032
$R_1/wR_2[I>2\sigma(I)]$	0.0312/0.0801	0.0458/0.1069
R_1/wR_2(all data)	0.0384/0.0836	0.0805/0.1214
Largest diff. peak/hole(e.Å^{-3})	0.657/-0.553	0.772/-0.434

Table 2 Crystal data and structure refinement parameters for compounds **11a-c**

	11a	**11b**	**11c**
Empirical formula	$C_{42}H_{44}Br_2N_4O_{21}S_2W_6$	$C_{46}H_{52}Br_2N_4O_{21}S_2W_6$	$C_{46}H_{52}Br_2N_4O_{21}S_2W_6$
Formula weight	2267.85	2323.94	2323.96
T (K), λ (Å)	298(2), 0.71073	298(2), 0.71073	298(2), 0.71073
Crystal system	triclinic	monoclinic	triclinic
Space group	*P-1*	$P2_1/c$	*P-1*
a(Å)	10.799(3)	10.371(4)	10.1433(12)
b(Å)	11.533(3)	12.851(5)	11.7753(14)
c(Å)	12.016(3)	21.899(8)	13.1042(16)
α(^{O})	117.088(4)	90.00	67.945(2)
β(^{O})	93.323(4)	93.172(7)	87.633(2)
γ(^{O})	90.887(4)	90.00	86.138(2)
V(Å^3)	1328.6(6)	2914.2(19)	1447.1(3)
Z, d_{calcd}(g cm^{-3})	1, 2.819	2, 2.642	2, 2.585
μ(mm^{-1}), F(000)	14.597, 1026	13.313, 2128	13.405, 1070
GooF on F^2	1.060	1.373	1.204
R_1/wR_2[I>2σ(I)]	0.0203/0.0509	0.0932/0.1750	0.0399/0.0847
R_1/wR_2(all data)	0.0232/0.0520	0.1032/0.1792	0.0442/0.0865
Largest diff. peak/hole(e.Å^{-3})	0.685/-0.884	1.852/-1.362	1.241/-1.134

Table 3 Crystal data and structure refinement parameters for compounds **11d-f**

	11d	**11e**	**11f**
Empirical formula	$C_{48}H_{48}Br_2N_4O_{21}S_2W_6$	$C_{48}H_{52}Br_2N_4O_{19}W_6$	$C_{56}H_{68}Br_2N_4O_{19}W_6$
Formula weight	2383.94	2251.86	2364.06
T (K), λ (Å)	298(2), 0.71073	298(2), 0.71073	298(2), 0.71073
Crystal system	monoclinic	triclinic	triclinic
Space group	$P2_1/c$	*P-1*	*P-1*
a(Å)	11.120(3)	9.9087(11)	11.2164(16)
b(Å)	12.375(3)	11.7099(13)	11.9454(17)
c(Å)	22.166(5)	12.4878(13)	12.8091(18)
α(^{O})	90.00	107.775(2)	76.337(2)
β(^{O})	99.222(4)	90.262(2)	85.806(2)
γ(^{O})	90.00	94.106(2)	70.853(2)
V(Å^3)	3010.9(12)	1375.7(3)	1575.4(4)
Z, d_{calcd}(g cm^{-3})	2, 2.585	1, 2.718	1, 2.492

μ(mm^{-1}), F(000)	12.887, 2156	14.020, 1034	12.250, 1098
GooF on F^2	1.022	0.990	1.317
$R_1/wR_2[I>2\sigma(I)]$	0.0316/0.0737	0.0431/0.0822	0.0554/0.0909
R_1/wR_2(all data)	0.0429/0.0787	0.0694/0.0909	0.0633/0.0933
Largest diff. peak/hole(e.Å^{-3})	1.470/-1.161	-0.771/0.176	1.073/-1.405

Table 4 Crystal data and structure refinement parameters for compounds **13a-c**

	13a	**13b**	**13c**
Empirical formula	$C_{58}H_{44}Br_2N_4O_{21}W_6$	$C_{66}H_{66}Br_2F_2N_4O_{23}S_4W_6$	$C_{58}H_{42}Br_2Cl_2N_4O_{19}W_6$
Formula weight	2363.89	2712.39	2432.78
T (K), λ (Å)	298(2), 0.71073	298(2), 0.71073	298(2), 0.71073
Crystal system	triclinic	triclinic	monoclinic
Space group	*P-1*	*P-1*	$P2_1/c$
a(Å)	9.4925(12)	11.628(3)	11.8559(12)
b(Å)	10.1101(12)	11.924(3)	12.5348(13)
c(Å)	15.7024(19)	15.585(4)	25.243(3)
α(^{O})	92.964(2)	92.288(4)	90.00
β(^{O})	100.955(2)	110.777(3)	97.995(2)
γ(^{O})	97.339(2)	109.182(3)	90.00
V(Å^3)	1462.9(3)	1878.1(7)	3714.9(7)
Z, d_{calcd}(g cm^{-3})	1, 2.683	1, 2.398	2, 2.175
μ(mm^{-1}), F(000)	13.192, 1086	10.407, 1270	10.463, 2236
GooF on F^2	1.219	1.115	0.987
$R_1/wR_2[I>2\sigma(I)]$	0.0355/0.0772	0.0593/0.1547	0.0403/0.0790
R_1/wR_2(all data)	0.0377/0.0782	0.0634/0.1575	0.0597/0.0841
Largest diff. peak/hole(e.Å^{-3})	0.0670/-1.705	2.439/-3.877	1.196/-0.799

Table 5 Crystal data and structure refinement parameters for **13d** and **13e**

	13d	**13e**
Empirical formula	$C_{58}H_{42}Br_4W_6N_4O_{19}$	$C_{68}H_{64}Br_2W_6N_4O_{19}$
Formula weight	2521.70	2504.15
T (K), λ (Å)	298(2), 0.71073	298(2), 0.71073
Crystal system	monoclinic	triclinic
Space group	$P2_1/c$	*P-1*
a(Å)	12.1119(15)	11.357(8)

b(Å)	12.3712(15)	12.033(8)
c(Å)	25.455(3)	16.571(11)
α(^{O})	90.00	81.165(11)
β(^{O})	97.635(2)	84.535(11)
γ(^{O})	90.00	75.025(11)
V(Å^3)	3780.3(8)	2158(3)
Z, d_{calcd}(g cm^{-3})	2, 2.215	1, 1.927
μ(mm^{-1}), F(000)	11.268	8.949, 1166
GooF on F^2	1.067	0.883
R_1/wR_2[I>2σ(I)]	0.0364/0.0775	0.0597/0.1333
R_1/wR_2(all data)	0.0497/0.0813	0.1085/0.1483
Largest diff. peak/hole(e.Å^{-3})	1.759/-1.673	2.275/-1.441

Table 6. Rotamers of the benzyl benzimidazolium cations and some geometrical parameters for the intermolecular stacking interactions in the relevant crystals.

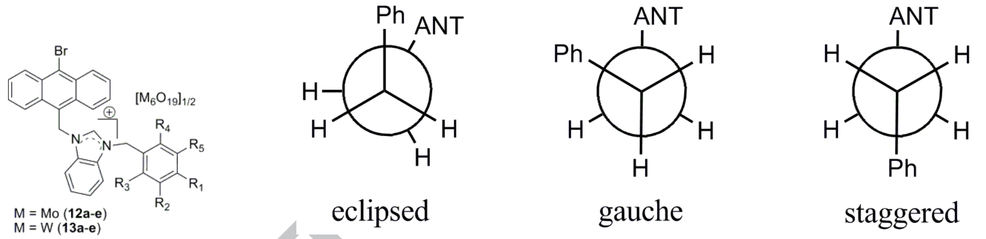

	Sp. Gr.	Geometry[a]	<(BIM–ANT)[b]	<(BIM–Ph)[c]	Torsion[d]
13a	*P–1*	eclipsed	82.48	80.50	19.95
13b	*P–1*	gauche	78.25	61.46	71.85
13c	$P2_1/c$	gauche	78.75	89.14	138.00
13d	$P2_1/c$	gauche	76.23	84.80	142.82
13e	*P–1*	eclipsed	76.55	88.37	106.11

[a] geometry of the benzyl benzimidazolium cations based on the spatial orientation of the phenyl and anthracene rings; [b, c] angle between the benzimidazole and anthracene plane and benzimidazole and phenyl plane respectively (°); [d]C(24)–C(23)–C(15)–C(14) dihedral angles(°).

Figure captions

Fig. 1. Thermal ellipsoidal plot of various ion pair compounds (as indicated by the numbers in the parentheses) in 20% probability. Only one cationic unit has been shown for clarity with various hydrogen bonding interactions between the different molecular components. Solvent molecules located in some of the structures have been excluded.

Fig. 2. Crystal structures of the compounds **11e–f** in 20% thermal probability distributions. Only one cationic unit has been displayed for clarity.

Fig. 3. ORTEP (20%) diagram of the compounds **13a**–**e**. Only one cation has been shown for clarity. Br(2) in the crystal structure of compound **13d** is disordered over two positions. However, in the relevant structural representation only one part has been shown.

Fig. 4. Pictures displaying basic intermolecular contacts between the components in the imidazolium cation containing solids.

Fig. 5. Newman projection for different orientations of the anthracene and phenyl rings of the benzimidazolium cations in the crystal structures of the compounds **13a**–**e** viewed down C(23)–C(15) axis. Solid bonds = atoms in front, hollow bonds = atoms at back.

Fig. 6. Portion of crystal packing in the lattice of the compounds **13a** (*P–1*) and **13a** ($P2_1/c$).

Fig. 7 Diffuse reflectance spectra (spread over $BaSO_4$) of the (a) various hexamolybdates containing N–alkyl imidazolium counter cations. The same feature has been observed in the benzimidazolium salts and has not been shown here. (b) bromide, hexamolybdate and hexatungstate salts of a same counter cation showing difference in spectroscopic behavior with the variation of the anion.

Fig. 1

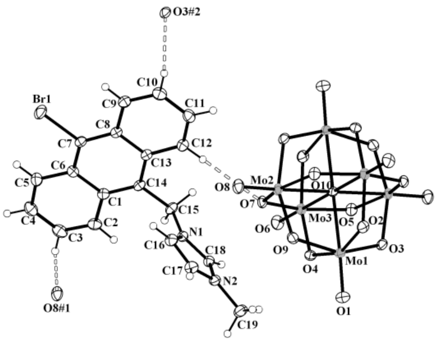

(**10a**)

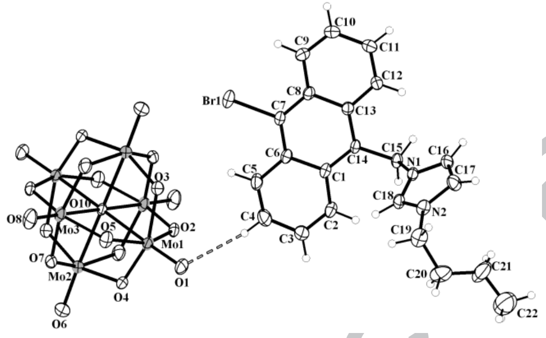

(**10d**)

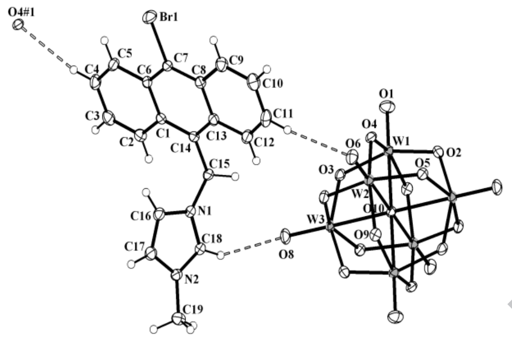

(**11a**)

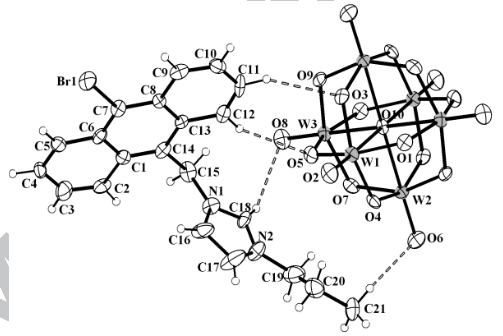

(**11b**)

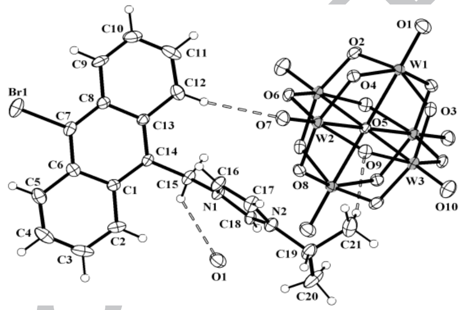

(**11c**)

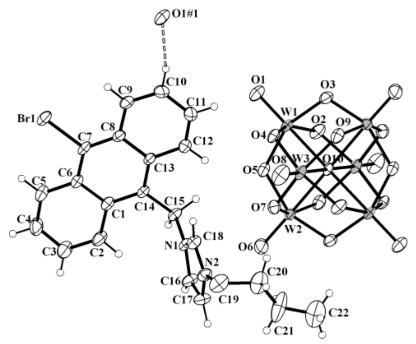

(**11d**)

Fig. 2

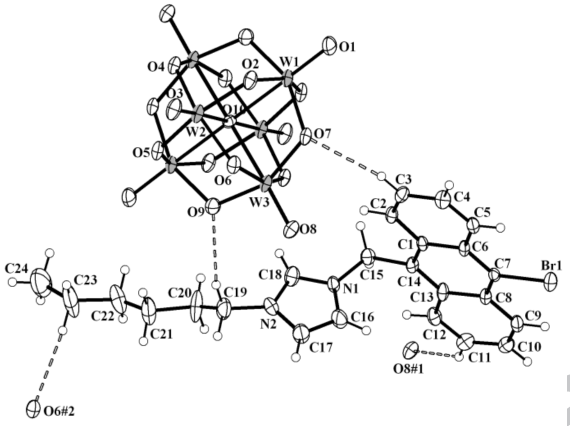
O4
O2
W1
O1
O3
O10
W2
O7
O5
O6
W3
O9
O8
C3
C4
C2
C5
C1
C6
C7
Br1
C15
C14
C13
C8
C24
C23
C20
C19
C18
N1
C9
C22
C21
N2
C16
C17
C12
C10
O8#1
C11
O6#2

(**11e**)

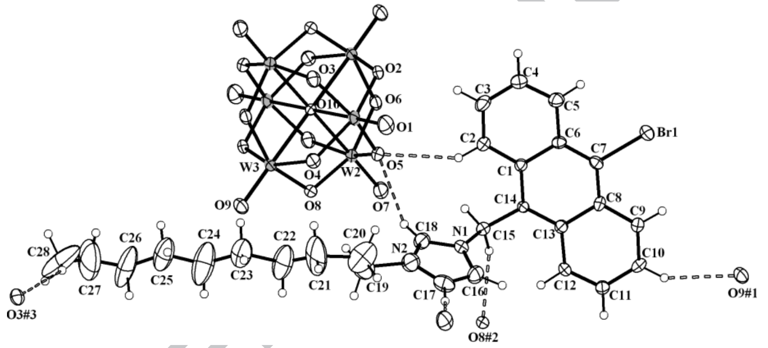
C4
O3
O2
C3
C5
O6
O10
O1
C6
C7
Br1
C2
W3
O4
W2
O5
C1
O9
O8
O7
C14
C8
C9
N1
C15
C18
C20
C13
C10
C28
C26
C24
C22
N2
C27
C25
C23
C21
C19
C17
C16
C12
C11
O9#1
O3#3
O8#2

(**11f**)

Fig. 3

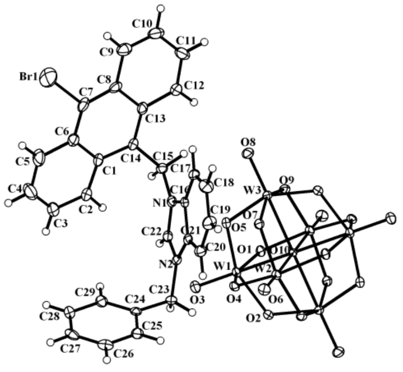

(**13a**)

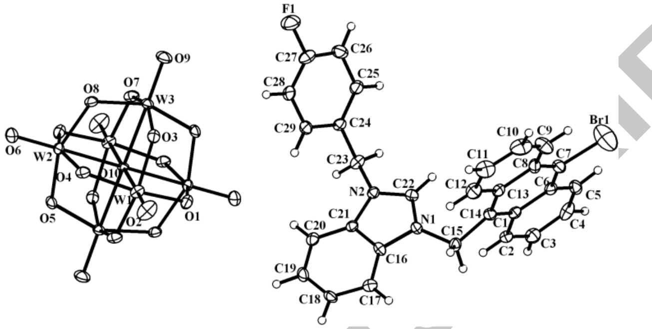

(**13b**)

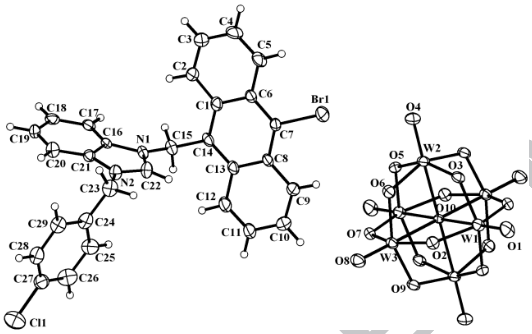

(**13c**)

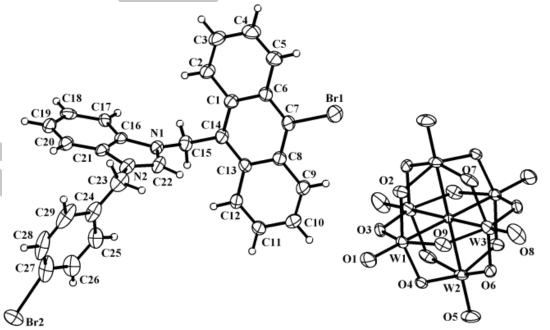

(**13d**)

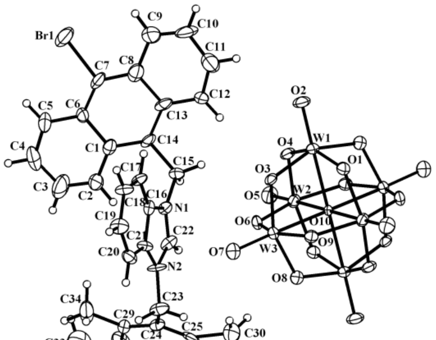

(**13e**)

Fig. 4

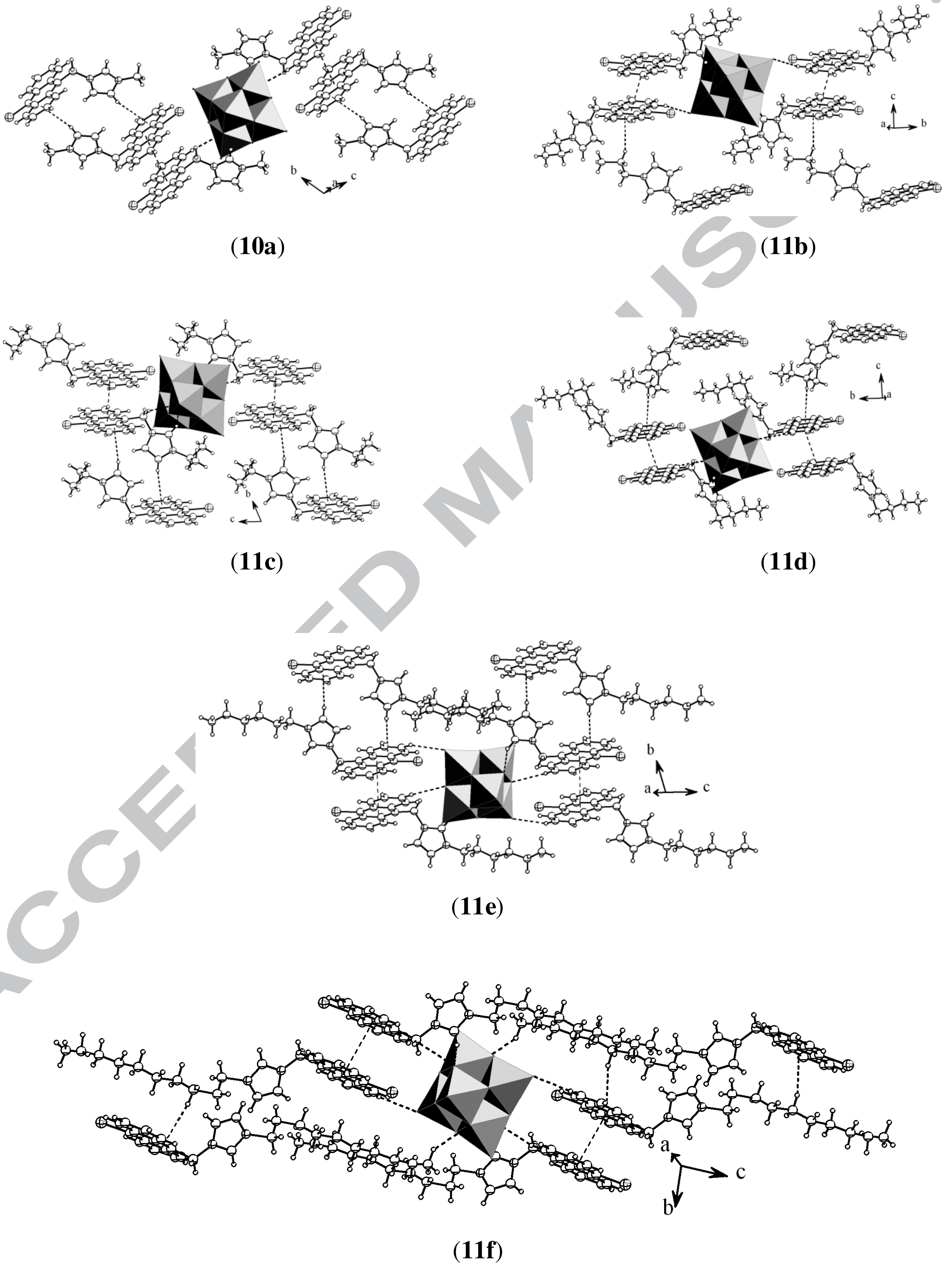

(**10a**) (**11b**)

(**11c**) (**11d**)

(**11e**)

(**11f**)

Fig. 5

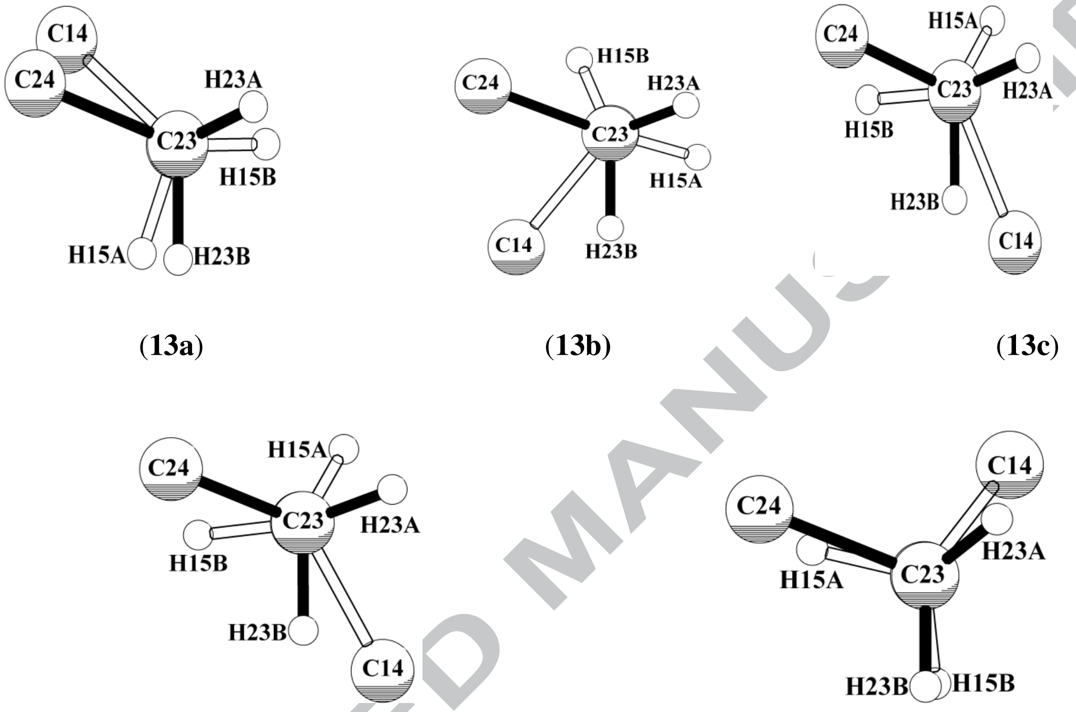

(**13a**) (**13b**) (**13c**)

(**13d**) (**13e**)

Fig. 6

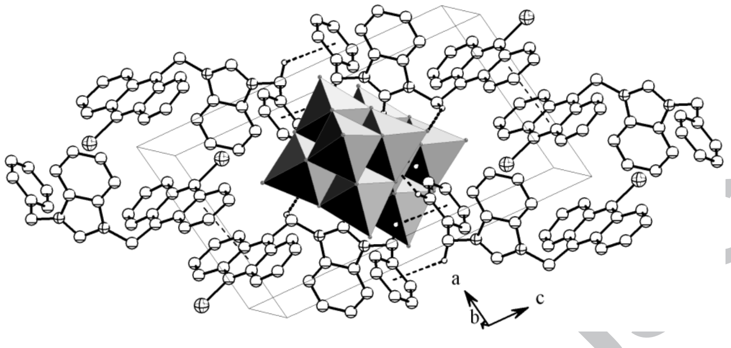

(**13a**)

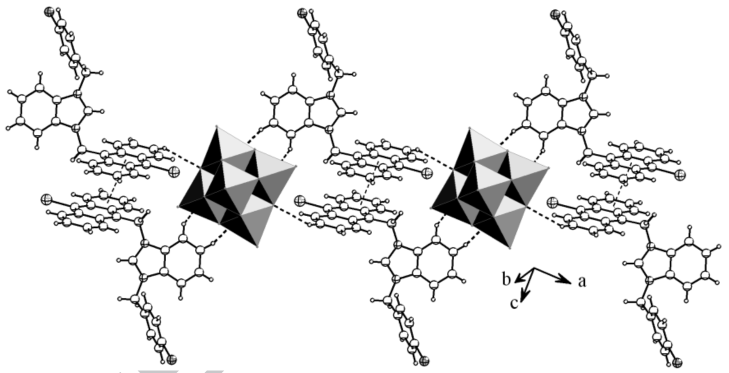

(**13c**)

Fig. 7

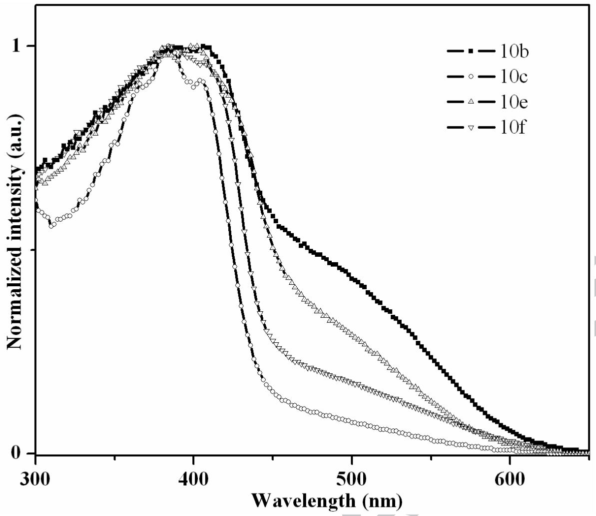

1
0
Normalized intensity (a.u.)
300
400
500
600
Wavelength (nm)
10b
10c
10e
10f

(a)

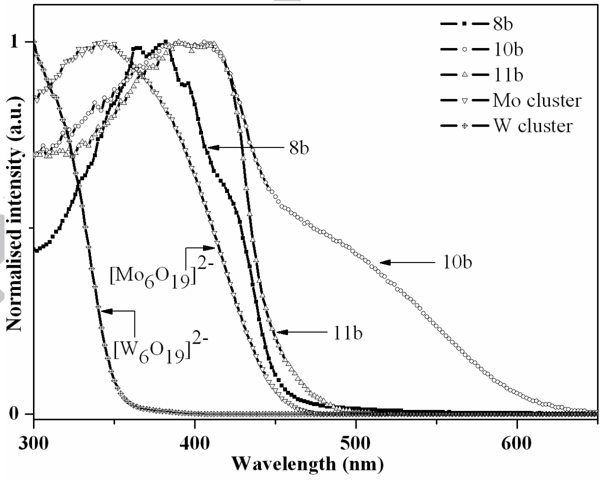

1
0
Normalised intensity (a.u.)
300
400
500
600
Wavelength (nm)
8b
10b
11b
Mo cluster
W cluster
8b
10b
11b
$[Mo_6O_{19}]^{2-}$
$[W_6O_{19}]^{2-}$

(b)

Artwork for TOC

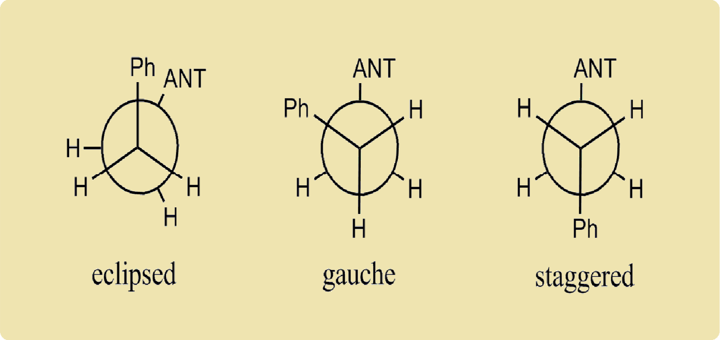

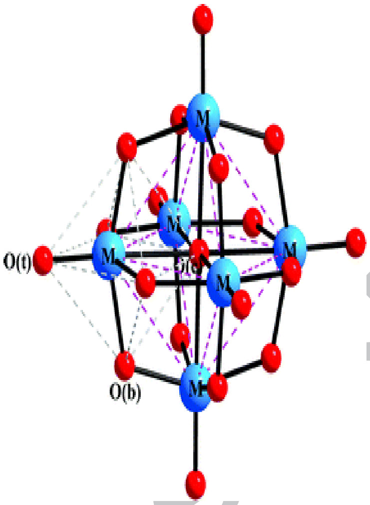

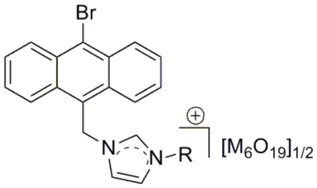

M = Mo (**10a-f**)
M = W (**11a-f**)

Text for TOC

Lindqvist type isopolyanions, namely, $[Mo_6O_{19}]^{2-}$ and $[W_6O_{19}]^{2-}$ as the counter anions can be associated with anthracene–imidazolium / anthracene-benzimidazolium cations to result in a series of Coulombic ion pair compounds that have been unambiguously determined by single crystal X–ray diffraction analysis. Even though, there is structural incompatibility between anthracene (planar) and the present polyoxometalate anions (spherical), Coulombic and several intermolecular weak interactions, e.g. C–H···O, C–H···π, π–π etc. compensate the destabilization energy, raised due to presence of the structurally mis-matched components in the respective crystal lattices.